

1. Report No. FHWA/LA-87/207	2. Government Accession No.	3. Recipient's Catalog No.	
4. Title and Subtitle EVALUATION OF EXPERIMENTAL INSTALLATION OF SILANE TREATMENT ON BRIDGES		5. Report Date April 1988	
		6. Performing Organization Code	
7. Author(s) Masood Rasoulia, Carl Burnett, Richard Desselles		8. Performing Organization Report No.	
9. Performing Organization Name and Address Louisiana Transportation Research Center 4101 Gourrier Avenue Baton Rouge, Louisiana 70808		10. Work Unit No.	
		11. Contract or Grant No. HPR 82-2C	
12. Sponsoring Agency Name and Address Louisiana Department of Transportation & Development P. O. Box 94245 Baton Rouge, Louisiana 70804		13. Type of Report and Period Covered Final Report September 1981 - April 1986	
		14. Sponsoring Agency Code	
15. Supplementary Notes Conducted in cooperation with the U.S. Department of Transportation, Federal Highway Administration.			
16. Abstract In this project the effectiveness of silane-based chemicals as concrete sealants was evaluated for selected bridges throughout the state of Louisiana for a five-year period. The field evaluation was initiated after satisfactory results in the laboratory. In conjunction with this study, Louisiana State University conducted an additional investigation on detection of silane reaction using infrared spectroscopy. The results obtained from the field study indicated that the silane-based chemicals provide some hydrophobic characteristics. The effects are not long-lasting and absorption decreased to 30% improvement over the untreated surface after four years. No changes in the chloride content or the corrosion activities were observed in treated or untreated bridges. The results of infrared spectroscopy indicated a depth of silane penetration of between 0 and 0.1" in the treated bridges.			
17. Key Words Concrete bridge deck, corrosion, moisture penetration, silane sealers		18. Distribution Statement No restriction. This document is available to the public through the National Technical Information Service, Springfield, VA 22161.	
19. Security Classif. (of this report) Unclassified	20. Security Classif. (of this page) Unclassified	21. No. of Pages 67	22. Price

EVALUATION OF EXPERIMENTAL INSTALLATION OF SILANE
TREATMENT ON BRIDGES

FINAL REPORT

BY

MASOOD RASOULIAN, P.E.
CONCRETE RESEARCH ADMINISTRATOR

CARL BURNETT
RESEARCH ENGINEER

AND

RICHARD DESSELLES
CONCRETE RESEARCH TECHNOLOGIST

CONDUCTED BY
LOUISIANA TRANSPORTATION RESEARCH CENTER
LOUISIANA DEPARTMENT OF TRANSPORTATION AND DEVELOPMENT

IN COOPERATION WITH

U.S. DEPARTMENT OF TRANSPORTATION
FEDERAL HIGHWAY ADMINISTRATION

The contents of this report reflect the views of the authors, who are responsible for the facts and the accuracy of the data presented herein. The contents do not necessarily reflect the official views or policies of the state or the Federal Highway Administration. This report does not constitute a standard, specification or regulation. The Louisiana Department of Transportation and Development and the Louisiana Transportation Research Center do not endorse products, equipment or manufacturers.

APRIL 1988

ACKNOWLEDGMENTS

Special appreciation is expressed to Dr. Harvill C. Eaton, Associate Dean, College of Engineering, Louisiana State University and Laura Clinton, graduate assistant at Louisiana State University, for the task of infrared spectroscopy analysis. A summary report is included in Appendix B.

ABSTRACT

In this project the effectiveness of silane-based chemicals as concrete sealants was evaluated for selected bridges throughout the state of Louisiana for a five-year period. The field evaluation was initiated after satisfactory results in the laboratory. In conjunction with this study, Louisiana State University conducted an additional investigation on detection of silane reaction using infrared spectroscopy.

The results obtained from the field absorption study indicated that the silane-based chemicals provide some hydrophobic characteristics. The effects are not long-lasting and absorption decreased to 30% improvement over the untreated surface after four years. No changes in the chloride content or the corrosion activities were observed in treated or untreated bridges. The results of infrared spectroscopy indicated a depth of silane penetration of between 0 and 0.1" in the treated bridges.

INTRODUCTION

Rainfall is the principal input to the hydrologic cycle, and its magnitude is a fundamental requirement of many hydrologic studies. Temporal and spatial characteristics of rainfall are needed to estimate runoff when rainfall-runoff models such as the Soil Conservation Service (SCS) method, rational method and others are used. Of practical necessity, rainfall is measured at a number of sample points. The amounts recorded at these points are then used to develop rainfall depths or intensity maps.

The most widely used source of rainfall of various durations and return periods is the U.S. Weather Bureau Technical Paper 40 (TP-40)(1), published in 1961. This rainfall atlas is based on the data prior to 1961, which makes it more than a quarter of a century old. Since then, over 30 years of additional data has become available but has not been used to update this widely used paper. Due to the relatively short period of records and the small number of rain gauges available at the time of preparation of TP-40, the desired accuracy and resolution was not obtained. Also the TP-40 maps consist of widespread contours and lack the details needed for more accurate design of drainage structures in a particular watershed, because these maps were developed for the entire country, not any particular state. The figure and equation numbers used in this summary are the same as in the final report.

BACKGROUND

The first extended rainfall frequency study in the United States was made by Yarnell (2) in the early 1930s and was presented in the form of maps for several combinations of return periods and durations for the continental United States. The U.S. Weather Bureau updated this work and published it as TP-40 (1) in 1961 with the use of additional rainfall data. This rainfall atlas contains 50 maps of the United States with contour lines of rainfall amounts for durations varying from 30 minutes to 24 hours and return periods from two to 100 years. A supplement to TP-40, HYDRO-35(3), was published by the National Oceanic and Atmospheric Administration (NOAA) of the National Weather Service (NWS) in 1977. This publication

provides rainfall contour maps for 5- to 60-minute durations and 2-, 10- and 100-year return periods for the Eastern and Central United States. This set of maps is a useful addition to TP-40 for estimating design storms of short durations or developing intensity-duration-frequency (I-D-F) charts. A literature survey relative to this topic revealed that a more detailed study to develop I-D-F charts was undertaken by Pennsylvania State University for the Pennsylvania Department of Transportation (4). A similar study was undertaken for the Arizona Department of Transportation (5). However, results of these studies are only applicable to those two states. The only published report with regard to precipitation in Louisiana was found to be Louisiana Rainfall (6), published by the Louisiana Department of Public Works in 1952. No reference on recent attempts to update Louisiana Rainfall or TP-40 for Louisiana was found.

OBJECTIVES OF RESEARCH

Objectives of this research were to develop maximum annual 24-hour rainfall maps and I-D-F curves for return periods of 2, 5, 10, 25, 50 and 100 years. Such rainfall information is used extensively for the design of highway drainage structures when a rainfall-runoff model is employed. Design rainfall is currently obtained from TP-40 (1), which is somewhat outdated. Another objective of this study was to assess the effect of errors in rainfall values and in model parameters on computed model output.

ANALYSIS OF RAINFALL DATA

Records were available for 92 rainfall observation stations in Louisiana for the period 1948-1987. Some of the stations had about 40 years of hourly rainfall records and some had shorter records, but almost every station had periods of missing records. The observation stations located in the same climatological region can be expected to have similar rainfall patterns. Therefore, the recorded rainfall values from nearby stations may be extrapolated from one station to another to fill data gaps. Before filling the data gaps, records must be analyzed to make sure that extrapolations are appropriate. The analyses of rainfall data involved the

following steps:

1. Data acquisition. Hourly precipitation data (TD-3240) was obtained from the National Climatic Data Center (NCDC) of the National Weather Service (NWS), U.S. Department of Commerce. TD-3240 contains records of 92 rain gauges in Louisiana.

2. Compilation and completeness of data. Extensive efforts were made for detailed examination of the raw data. The collected data was a combination of original observations of hourly and accumulated precipitation. The original data was labeled with measurement flags of A for accumulated values, M for missing values, and D for deleted values. A, M, and D values should come in pairs, with the first date indicating the beginning and the second date the end of the period. However, some of these records were found not to come in pairs. Therefore, a computer program (RAINAMD) was developed to check for flagged unpaired records. Erroneous records were then deleted from the data set. A computer program (RAINST) was also developed to compute rainfall values for designated stations within a designated time period. If rainfall values were missing, deleted or accumulated over several hours, an attempt was made to calculate those values using data from other selected stations. In order to provide a long period of records for a reliable statistical analysis records at stations located within a 10-mile radius were combined when a single station with a long record was not present. This grouping of rain gauges provided 26 synthesized (representative) stations. The 26 synthesized stations are shown in Figure 2.1. The stations that comprised a synthesized station were called primary stations. The stations that were not primary stations to a synthesized station were called secondary stations.

3. Tests for homogeneity of data. The appropriateness of the data synthesis was checked by the correlation plottings of monthly rainfall between the rain gauges to make sure that the homogeneity property was not severely violated. Correlation plots consisted of plots between primary and primary, primary and secondary, primary and synthesized, and synthesized and synthesized stations. Once the homogeneity test was performed, the station with the longest record length and the least number of missing data was selected as the "basic" station to form

the synthesized station record. Rainfall values from other stations within the primary group were used to fill data gaps. Normally, more than one station was used. If missing records of the synthesized station could not be filled completely from primary stations, the missing data were filled using values from nearby secondary stations which demonstrated a strong correlation with the "basic" station. Inverse distance squared method was used to fill in the missing data from the nearby secondary stations.

4. Testing the completion of data. In order to check the overall process of data completion, accumulated recorded and synthesized rainfall values were compared for the entire period of records at all stations. Mass curves were also developed to see if the cumulative rainfall values from 26 synthesized stations were reasonably close to those recorded .

5. Computation of annual maximum rainfall depths for selected durations. With 26 complete data sets representing the 26 synthesized stations, the annual maximum 24-hour rainfall depth series at each synthesized station was calculated using the computer program RAINFALL.FORTRAN. This was done by inserting zero values for non-rainfall hours to make the rainfall data continuous, then scanning the continuous data and finding the maximum 24-hour annual rainfall depth. The annual maximum rainfall depths for the durations of 1, 3, 6, 12, 36, 48, 60, 72, and 96 hours were also calculated for all of the 26 stations, which were used for developing the I-D-F curves.

SELECTION OF DISTRIBUTION AND PARAMETER ESTIMATION METHOD

The objective of rainfall frequency analysis is to estimate the quantiles of extreme rainfall or rainfall intensity for a given duration and return period. Then the flood quantiles of a stream can be obtained by using a selected rainfall-runoff model.

The quantile estimates at any site are subject to considerable inherent variability (7). The major factors that affect the extent of variability are: (a) the sample size of an observation station; (b) the recurrence interval of estimate; (c) the population distribution selected; and

(d) the parameter estimation method used. Because there exist vast possible hydrogeological variations in time and space, the population distribution may have a remarkably wide range of forms for various sites. The choice of a probability distribution from many candidate probability distributions is compounded by the limited amount of available data.

Several studies have been reported in the literature to compare the performance of various distributions with various parameter estimation methods. Kuczera (8) compared six distributions using different parameter estimation methods, i.e., (a) normal distribution with maximum likelihood estimation (MLE); (b) two-parameter log-normal (LNO2) distribution with MLE, and method of moments (MOM); (c) log-Pearson type 3 (LPEAR3) with the indirect method of moment (MMI) estimation, the method recommended by U.S. Water Resources Council (USWRC) (9); (d) extreme value type 1 (EV1) distribution with MLE, probability weighted moments (PWM) and MOM; (e) log-EV1 distribution with MOM; and (f) Wakeby distribution (WAK) with PWM. Wallis and Wood (10) compared the performance of the general extreme value (GEV) distribution with PWM, the WAK distribution with PWM, and the LPEAR3 with MMI. Arora and Singh (7, 11) compared EV1 with MOM, MLE, PWM, mixed moments (MIX), maximum entropy method (ENT), least squares and incomplete means by Monte Carlo simulation, and LPEAR3 with MOM, MMI, MIX, MLE, and ENT. However, there is no general consensus on either the performance of specific distribution or a specific parameter estimation method. For example, Arora and Singh (7) concluded, based on their Monte Carlo simulation results, that the LPEAR3 with MMI performed poorly and suggested a revision of the recommendation by USWRC (9) of using LPEAR3-MMI; while others found LPEAR3-MMI gave relatively better quantile predictions (9, 12).

A quantitative approach for selection of an appropriate distribution and parameter estimation method is to test some of the most frequently used distributions in applied hydrology along with the most robust parameter estimation methods. Using certain statistics criteria such as mean square error and bias, one can compare the performances of different combinations of the distributions and estimation methods and select the best combination.

In this study, five popular distributions and three parameter estimation methods widely used in applied hydrology were considered for a comparative analysis. The five probability distributions are:

1. 2-parameter log-normal (LNO2)
2. 3-parameter log-normal (LNO3)
3. Pearson type 3 (PEAR3)
4. log-Pearson type 3 (LPEAR3)
5. Extreme-value type 1 (GUMBEL)

The three parameter estimation methods are:

1. Method of moments (MOM)
2. Maximum-likelihood estimate (MLE)
3. Principle of Maximum entropy (POME)

A comprehensive FORTRAN computer program, FREQUENT.PROG, was developed to perform the following tasks:

1. To estimate the parameters of the five distributions by three estimation methods, using the annual maximum rainfall series of each of the 26 synthesized stations.
2. To compute the relative mean square error for all combinations of distributions and estimation methods at each station.
3. To compute the average MSE for all combinations of distribution and methods over 26 stations using the annual maximum rainfall series.
4. To compute the relative bias for all combinations of distributions and estimation methods at each station.
5. To compute the average BIAS for all combinations of distributions and methods over the 26 stations using the annual maximum rainfall series.

6. To generate rainfall quantiles for each of the 26 stations corresponding to 11 durations (1, 3, 6, 12, 24, 36, 48, 60, 72, 84 and 96 hours) with six return periods (2, 5, 10, 25, 50 and 100 years). The 24-hour quantiles were used to develop the isohyetal maps.

7. To generate rainfall-intensity quantiles for 26 stations corresponding to 11 durations (1, 3, 6, 12, 24, 36, 48, 60, 72, 84 and 96 hours) and six return periods (2, 5, 10, 25, 50 and 100 years) for development of I-D-F curves.

Note that the mean square error (MSE) computed in all tables are standardized values. The MSE at each station for a selected rainfall duration is defined as

$$\text{MSE} = \frac{1}{n} \sum_{i=1}^n \left[\frac{x_c(i) - x_o(i)}{\bar{x}} \right]^2 \quad (3.71)$$

where $x_c(i)$ and $x_o(i)$ are the computed and observed rainfall values at the i -th plotting position, and \bar{x} is the sample mean at the same station. Similarly, the standardized bias (BIAS) at a station for a selected rainfall duration is defined as

$$\text{BIAS} = \frac{1}{n} \sum_{i=1}^n \left[\frac{x_c(i) - x_o(i)}{\bar{x}} \right] \quad (3.72)$$

Computed results showed that the best combinations for each station are LPEAR3-MOM(19), EV1-MLE(2), LPEAR3-POME(2), PEAR3-MOM(1), LNO3-MOM(1) and LPEAR3-MLE(1), where the number in the parenthesis is the number of times that the combination gives the smallest MSE. Thus, LPEAR3-MOM is the preferred combinations for 19 out of 26 stations. However, LNO3-MLE yields the smallest BIAS values for 25 stations with one station having the smallest BIAS by LPEAR3-MOM. Therefore, LNO3-MLE may be selected as the best combination of distribution and method if the BIAS is used as the performance index. In practice, however, MSE is usually considered to be a more important performance index than

BIAS while the corresponding BIAS is not excessively large. Since the LPEAR3-MOM has the smallest average MSE with the corresponding BIAS comparable to other methods, LPEAR3-MOM is selected as the most appropriate combination of distribution and estimation method for the Louisiana rainfall data.

DEVELOPMENT OF THE 24-HOUR ISOHYETAL MAPS

Rainfall quantiles for the 26 stations for 11 durations (1 through 96 hours) were computed using LPEAR3 distribution with the MOM estimation method. Since the observed data sets may contain various errors and may have various lengths of missing records, the estimated quantiles would inevitably contain errors and uncertainties. It was observed that the computed quantiles often changed abruptly from one station to another. Therefore, proper care must be taken for drawing the isohyetal maps. Several rules were devised to make these drawings meaningful.

First, the means of the quantile values were computed from each one-degree quadrangle of latitude and longitude to filter out possible random errors. The "initial" 24-hour isohyetal curves for various return periods were drawn based on these average values. However, many other types of errors exist which may render the "initial" isohyetal curves unacceptable. As a result, these curves have no distinct pattern and sometimes even intersect each other. To improve the "initial" curves, the following rules were applied:

1. If a station quantile in a one-degree quadrangle deviates from its mean by three standard deviations, that quantile is eliminated from the computed data set.
2. If only one or two stations exist in a one-degree quadrangle, adjacent station values are used to compute the mean value.
3. If a station is located between two adjacent one-degree quadrangles, the quantile at that station is used in computations by both one-degree quadrangle.

4. At the corner quadrangles where the trend of the isohyetal lines is unclear, nearby individual station values are given higher importance than average values.
5. When the isohyetal curves changes drastically in a small local area, the curve is modified based on the nearby curve pattern, geographical and climatological conditions, or the reliability of the nearby station data. This is necessary to provide smooth transitions for the isohyetal curves.

The final 24-hour isohyetal curves for the return periods $T = 2, 5, 10, 25, 50,$ and 100 years, were drawn based on the above rules and are shown in Figures 4.1 through 4.6.

A comparison was made between the newly-developed isohyetal maps ("newmap") and TP-40 for the return periods of 2, 5, 10, 25, 50 and 100 years. The performance indice MSE and BIAS defined by Equations (3.71) and (3.72) were used for the comparison. MSE and BIAS were computed using values from each map at the corresponding stations. In general, for return periods of less than or equal to 25 years, the newly-developed isohyetal maps are superior to the TP-40 maps in terms of both MSE and BIAS. For return periods of 50 and 100 years, the newly-developed maps are significantly superior to the TP-40 maps in terms of MSE, but have slightly larger BIAS.

On the average, for all of the 26 synthesized stations corresponding to six return periods, the new maps reduced the MSE by 58 percent and the BIAS by 80 percent, as compared to the TP-40 maps. Thus, the new isohyetal maps greatly improved the accuracy of the old maps based on the available observed station data.

DEVELOPMENT OF I-D-F CURVES

At each synthesized station, the 1-, 3-, 6-, 12-, 24-, 36-, 48-, 60-, 72-, 84- and 96-hour quantiles for six return periods ($T = 2, 5, 10, 25, 50$ and 100 years) were calculated by the computer programs RAINFALL.FORTRAN and FREQUENT.PROG. The corresponding rainfall-

intensity quantiles for the above 11 durations and six return periods were also generated using the LPEAR3 distribution in conjunction with the method of moments for parameter estimation for all 26 stations. With these computed rainfall-intensity quantiles for the five durations at each station for each return period, one can fit a model using a non-linear least squares method. The SAS (21) non-linear regression routine was used to fit a model to the computed quantiles. Several models were tested and the following three-parameter non-linear model was selected.

$$I = a (D + b)^c \quad (5.1)$$

where a, b and c are three constant parameters, I is the rainfall intensity (inches/hour) for a given return period and D is the rainfall duration (hours). The parameters at each station and for different return periods for all 26 stations were computed and are listed in Tables 5.1 through 5.6. These parameters changed a great deal from station to station within a given return period. This variation of parameters got larger for higher return periods. Thus, the I-D-F curves or regression models developed for each single station only represent the estimate of the intensity quantile for a given duration and return period for the immediate vicinity of that station rather than the region. For design purposes, station parameters may be used with Equation (5.1) to estimate rainfall intensities when study sites are near the station.

ERROR ANALYSIS

Error analysis deals with effects of errors resulting from various sources on model output (22). Four sources of errors were listed by Neumann and Goldstein (23): (a) mathematical models are approximate or idealized representations of physical systems; (b) model parameters are estimated from experimental or historical data and are subject to data and estimation errors; (c) model solutions may involve truncation errors; and (d) numerical computation involves round off errors. In addition, (e) a model may directly contain an input component which is subject to reading errors, data operation errors, as well as instrumental errors. Of these sources, errors from source (a), (b) and (e) are most significant.

In frequency analysis, two types of mathematical models have to be developed. First, a proper frequency distribution has to be selected for the purpose of frequency analysis; and second, a proper rainfall-runoff model has to be selected for the study of the rainfall-runoff relationship for a given probability. Once the models are selected, parameters in these models are calibrated using the observed data. The model selection, calibration and prediction for rainfall-frequency analysis have been discussed. However, there are uncertainties or errors involved in these selected models that must be recognized. Moreover, error from estimated parameters and error from input component should be analyzed before any application. Sensitivity analyses are usually used for this purpose. The first-order analysis of uncertainty can be employed to quantify the expected variability arising from uncertainty in parameters and input components.

In this study, we follow the procedure of first-order analysis outlined by Singh and Yu (24). Errors in rainfall values may arise due to improper description or measurement of rainfall, whereas errors in parameters may be due to lumping spatial variability of the parameters and inadequate characterization of the land use and soil-vegetation complex. When using the SCS model errors in runoff volume were assessed by varying the rainfall and keeping the parameter associated with the land use, the curve number (CN), fixed. Then the effect of the CN on runoff volume and subsequently on the peak rate of runoff was analyzed by varying the CN and keeping the rainfall input fixed. The same methodology was also applied to parameters of the selected frequency distribution, namely, the LP3 distribution. These analyses demonstrate the sensitivity of runoff to different model parameters and model input component. By this type of sensitivity analysis one can clearly know which parameter or component needs to be evaluated more accurately than others.

Based on the estimated parameters from the annual maximum 24-hour rainfall at Station 1 for a return period of 50 years, it was found that the output error is most sensitive to errors in parameter \bar{y} , less sensitive to parameter S_y , and least sensitive to parameter G_y . This is a positive outcome since the accuracy of estimating these three parameters rank in reverse order of the sensitivity analysis. That is why the moment-based methods of parameter estimation often

yields better results. An error analysis was also made to assess the effect on computed runoff values due to errors in parameters and rainfall input for the SCS rainfall-runoff model. Computed results showed that the SCS rainfall-runoff model is equally sensitive to both parameters CN and rainfall input component P.

SIGNIFICANCE OF RESEARCH

There are many instances in highway design when runoff for drainage structures must be estimated for gauged as well as ungauged sites. The accuracy of available methodologies highly depends on reliable inputs of rainfall values. Therefore, existing outdated rainfall information needs to be updated frequently. Results of this research work are expected to enhance the accuracy of the existing rainfall information for Louisiana through the use of longer records of rainfall data and a larger number of rain gauges. These maps will be used for: (a) more reliable design of highway drainage structures; (b) highway planning; (c) damage assessment; and (d) effect of land-use change. It is anticipated that the findings of this study will permit more reliable design of highway drainage structures, resulting in savings in both construction and maintenance.

IMPLEMENTATION

The new 24-hour rainfall frequency maps and Intensity-Duration-Frequency (I-D-F) curves developed in this study have been derived using records of 92 rain gauges in Louisiana for the period from 1948 to 1987. The new rainfall maps and I-D-F- curves, which will provide LaDOTD with the most up-to-date information on rainfall in Louisiana, will replace the ones currently used by the design personnel of LaDOTD.

There appears to be no costs associated with the implementation of the new rainfall maps and I-D-F curves; therefore, they can be immediately implemented in the LaDOTD Hydraulics Manual.

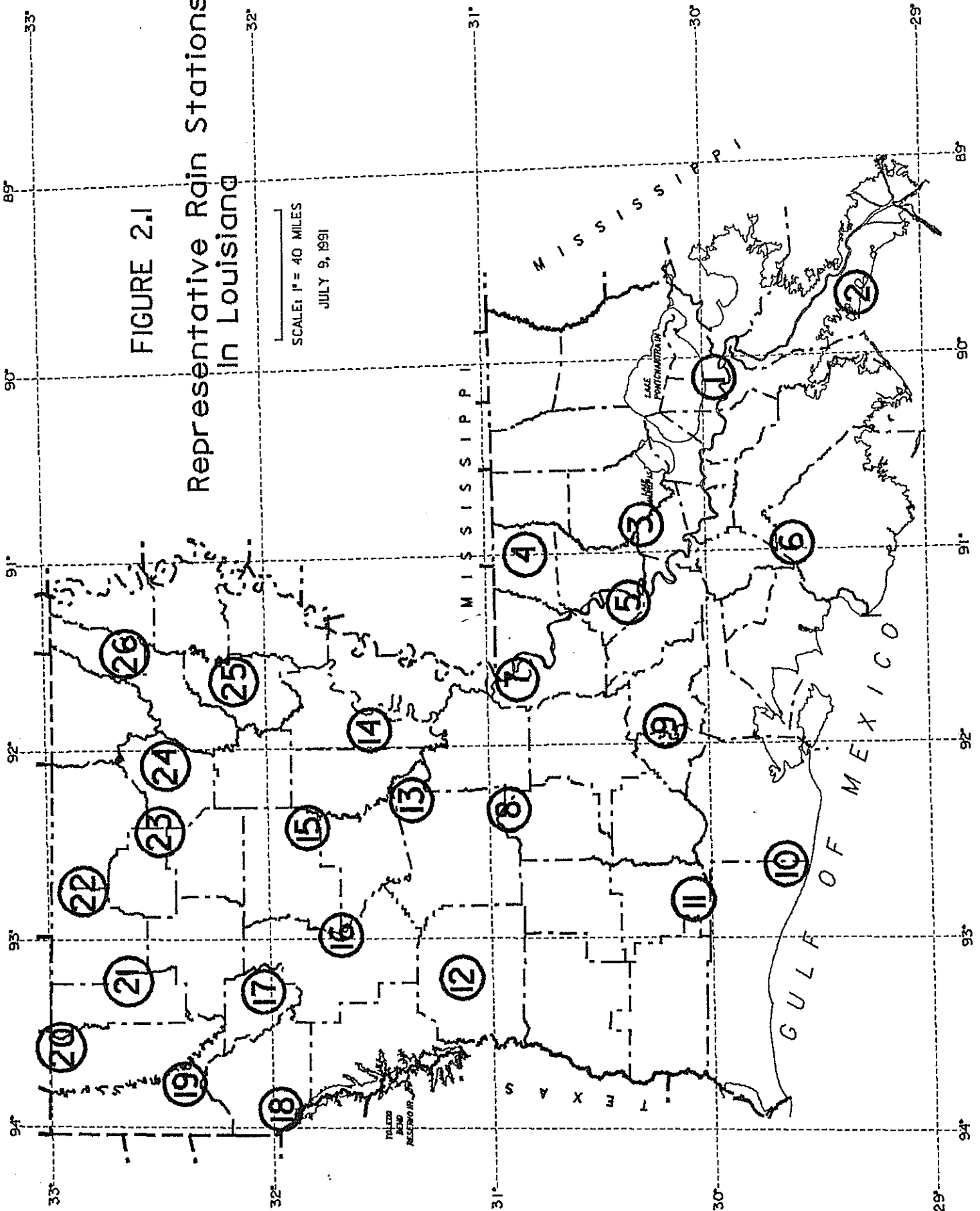
REFERENCES

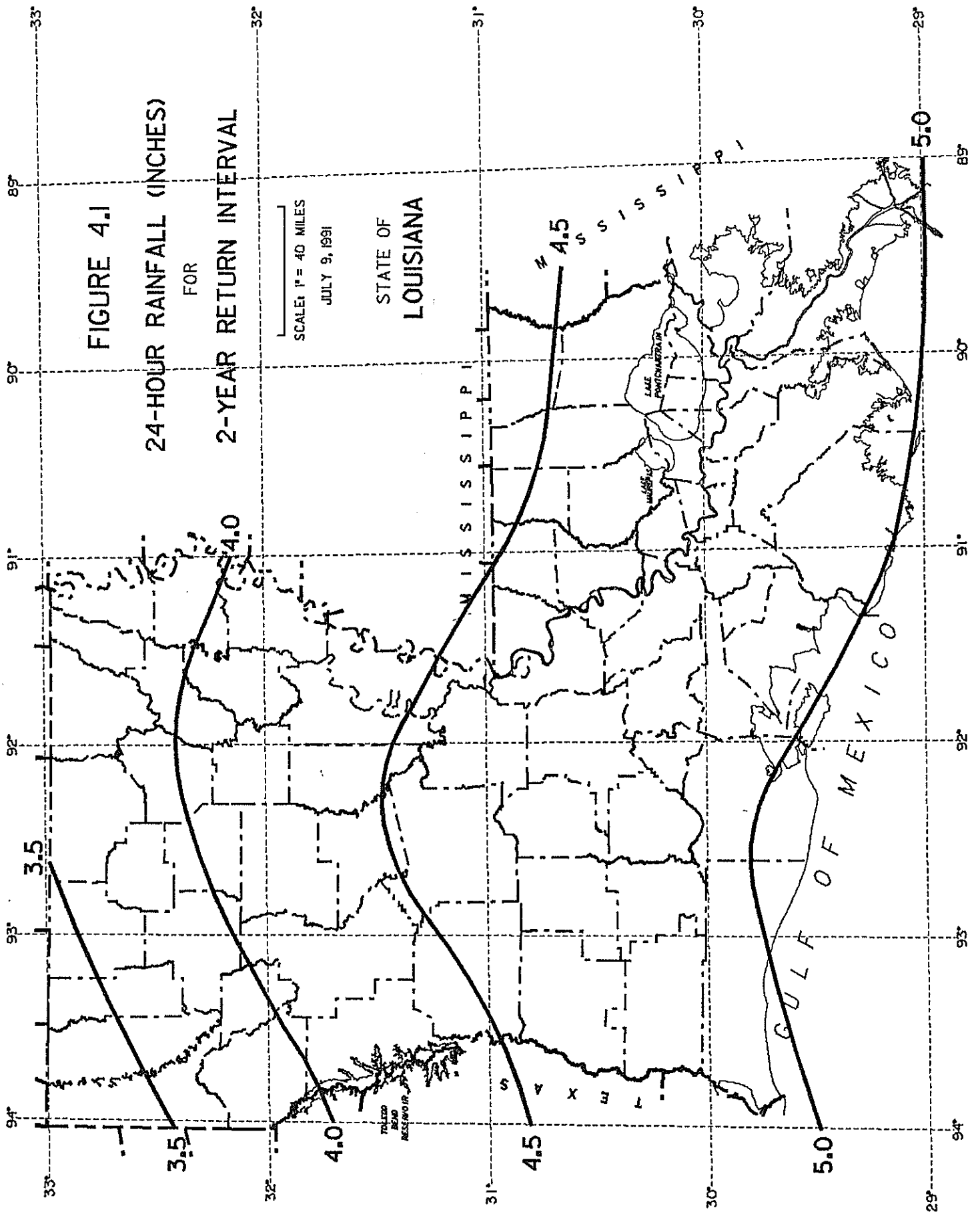
1. "Rainfall Frequency Atlas of the United States," Technical Paper No. 40, U.S. Department of Commerce, Washington, D.C., 1961.
2. Yarnell, D. L., "Rainfall-Intensity-Frequency Data", Miscellaneous Publications No. 204, U.S. Department of Agriculture, Washington, D.C., 1935.
3. "Five- to 60-Minute Precipitation Frequency for the Eastern and Central United States," NOAA Technical Memorandum NWS HYDRO-35, National Weather Service, Silver Spring, Maryland., 1977.
4. Aron, G., et al., Pennsylvania Department of Transportation Storm Intensity-Duration-Frequency Charts, FHWA-PA-85-032, Pennsylvania State University, University Park, Pennsylvania, 1986.
5. "Storm Rainfall Probability Atlas for Arizona," FHWA-AZ88-276, Arizona Department of Transportation, Phoenix, Arizona, 1988.
6. Louisiana Rainfall, Intensity-Duration-Frequency Data and Depth-Area-Duration Data, Department of Public Works, Baton Rouge, Louisiana, 1952.
7. Arora, K. and Singh, V. P., "A Comparative Evaluation of the Estimators of the Log Pearson Type 3 Distribution," Journal of Hydrology, Vol. 105, 1989, pp. 19-37.
8. Kuczera, G., "Robust Flood Frequency Models," Water Resources Research, Vol. 18, No. 2, 1982, pp. 315-324.
9. U.S. Water Resources Council, "Guidelines for Determining Flood Flow Frequency," Hydrology Subcommittee, Bulletin #15, Washington, D.C., 1967.
10. Wallis, J. R., and Wood, E. F., "Relative Accuracy of Log Pearson III Procedures," Journal of the Hydraulics Division, ASCE, Vol. 111, No. HY7, 1985, pp. 1043-1056.
11. Arora, K. and Singh, V. P., "On Statistical Intercomparison of EVI Estimates by Monte Carlo Simulation," Advanced Water Resources, Vol. 10, 1987, pp. 87-107.
12. Jain, D. and Singh, V. P., "Comparison of Some Flood Frequency Distributions Using Empirical Data," Hydrologic Frequency Modeling, V. P. Singh (editor), D. Reidel Co., Germany, 1987, pp. 467-485.
13. Kite, G. W., Frequency and Risk Analysis in Hydrology, Water Resources Publications, P. O. Box 303, Fort Collins, Colorado 80522, 1978.

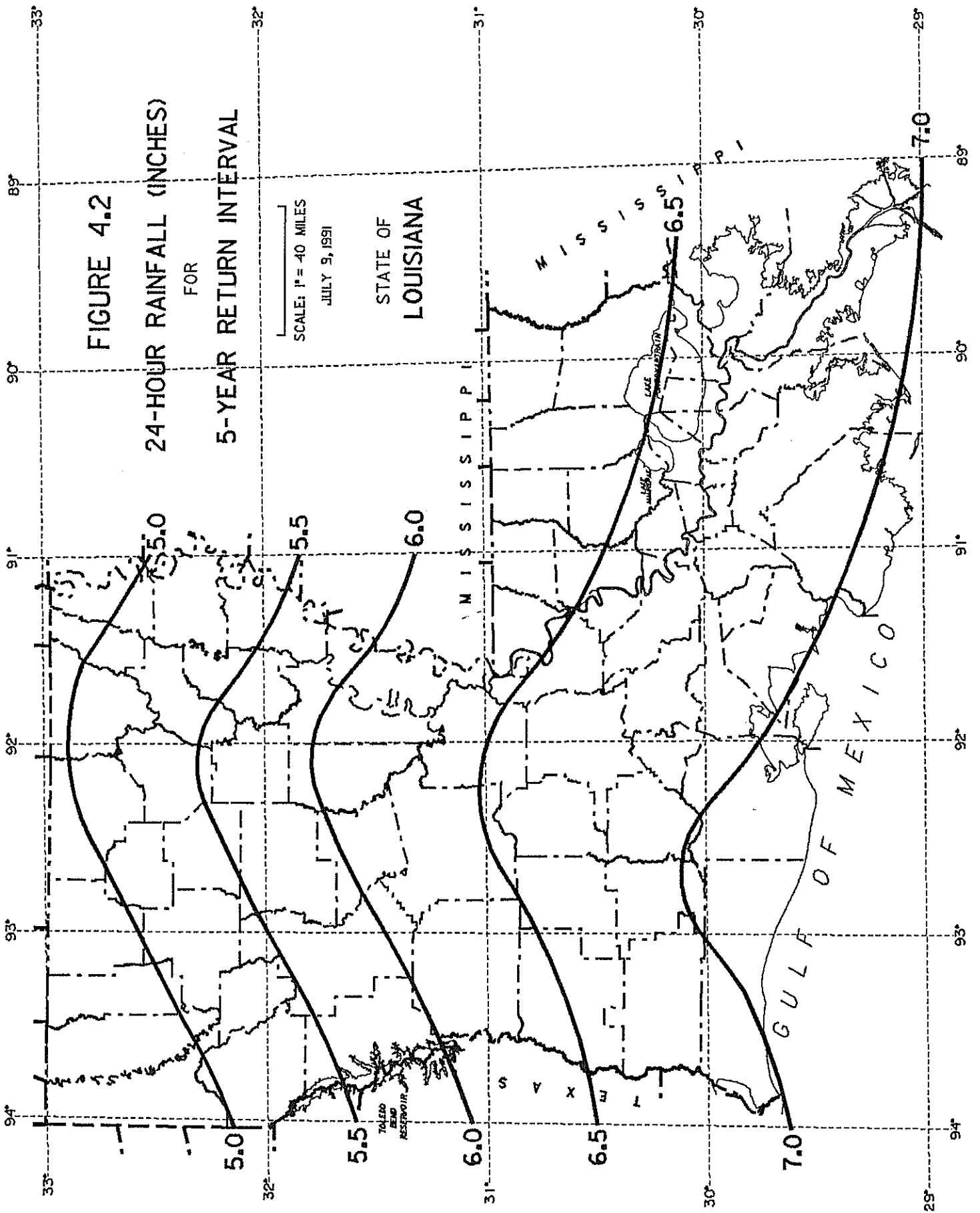
14. Singh, V. P.; Rajagopal A. K.; and Singh, K., "Derivation of Some Frequency Distributions Using the Principle of Maximum Entropy (POME)", *Advanced Water Resources*, Vol. 9, 1986, pp. 91-106.
15. Condie, R. and Nix, G., "Modeling of Low Flow Frequency Distributions and Parameter Estimation," *International Water Resources Association, Proceedings of Symposium on Water for Arid Lands*, Tehran, Dec. 8-9, 1975.
16. Matalas, N. C. and Wallis, J. R., "Eureka, It Fits a Pearson Type 3 Distribution," *Water Resources Research*, Vol. 9, No. 2, 1973, pp. 281-289.
17. Reich, B. M., "Log-Pearson Type 3 and Gumbel Analysis for Floods," *Second International Symposium in Hydrology*, Fort Collins, Colorado, 1972, pp. 290-303.
18. Bobee, B., "The Log-Pearson Type 3 Distribution and its Application in Hydrology," *Water Resources Research*, Vol. 11, No. 5, 1975, pp. 681-689.
19. Rao, D.V., "Log-Pearson Type 3 Distribution: A Generalized Evaluation," *Journal of Hydraulic Engineering*, ASCE, Vol. 106, No. 5, 1980, pp. 853-872.
20. Bobee, B. and Robitaille, R., "The Use of Pearson Type 3 and Log-Pearson Type 3 Distribution Revisited," *Water Resources Research*, Vol. 13, No. 2, 1976, pp. 427-443.
21. SAS User's Guide, Version 5 Edition, SAS Institute Inc., Cary, NC., 1989.
22. Singh, V.P., Hydrologic Systems, Volume I, Rainfall-Runoff Modeling, Prentice Hall, Englewood Cliffs, New Jersey, 1988.
23. Von Neumann, J. and Goldstine, J. J., "Numerical Inverting of Matrices of High Order," *Bulletin of the American Mathematical Society*, Vol. 53, 1947, pp. 1021-99.
24. Singh, V. P. and Yu, F. X., "Derivation of an Infiltration Equation Using Systems Approach," *Journal of Irrigation and Drainage Engineering*, ASCE, Vol. 116, No. 6, 1990, pp. 837-858.
25. Soil Conservation Service National Engineering Handbook, Section 4, Hydrology, U.S. Soil Conservation Service, 1972.

FIGURE 2.1
Representative Rain Stations
In Louisiana

SCALE: 1" = 40 MILES
JULY 9, 1991







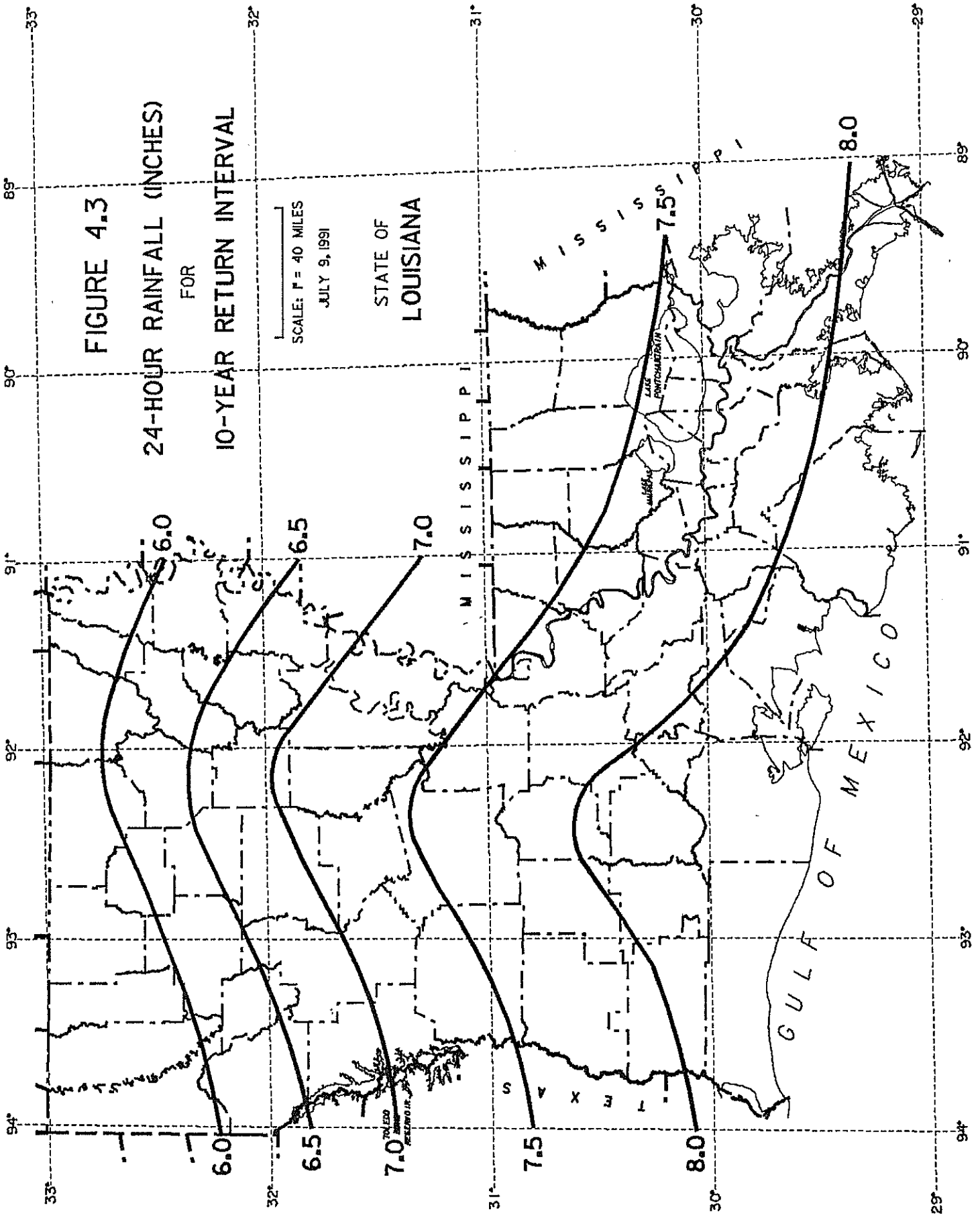
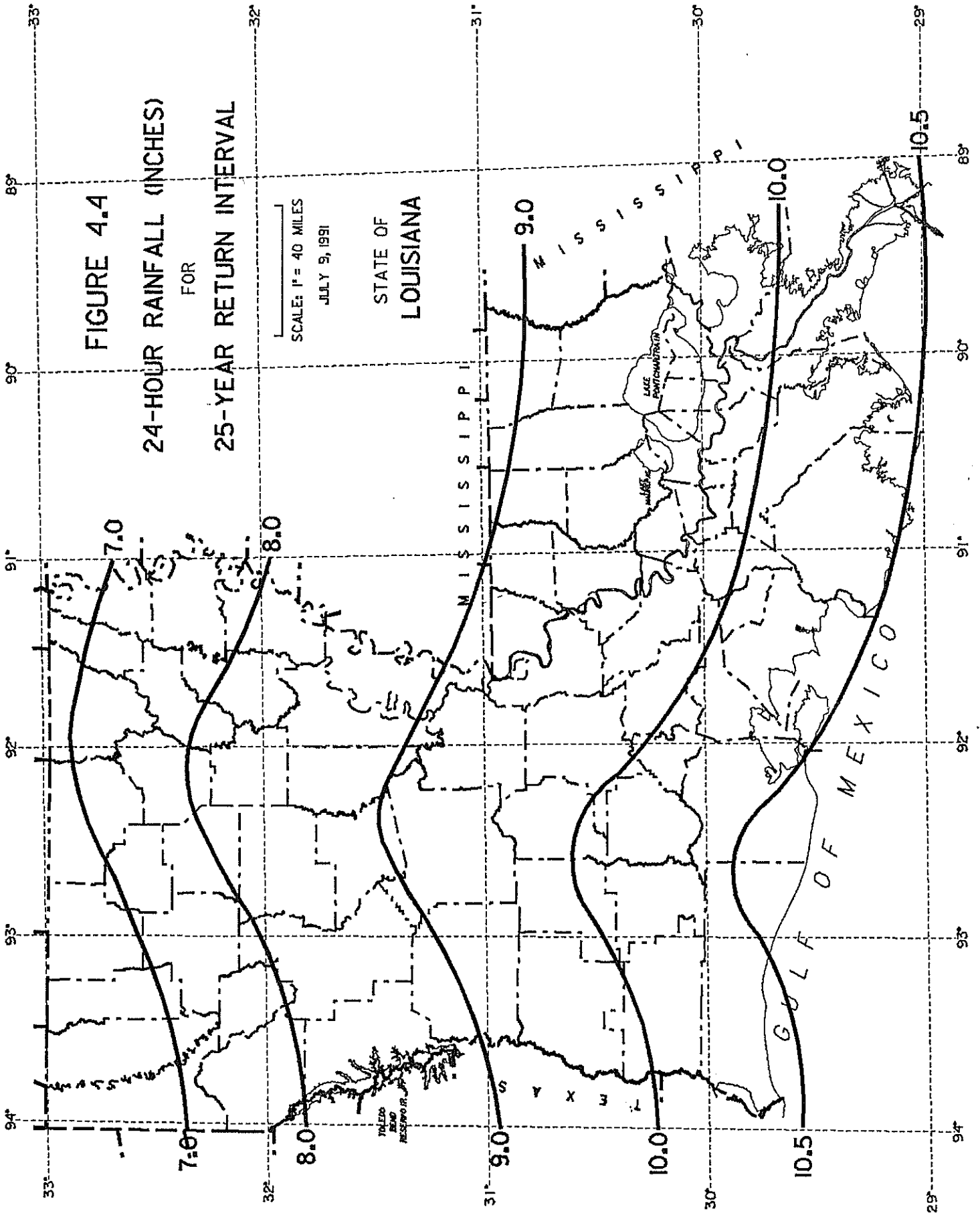
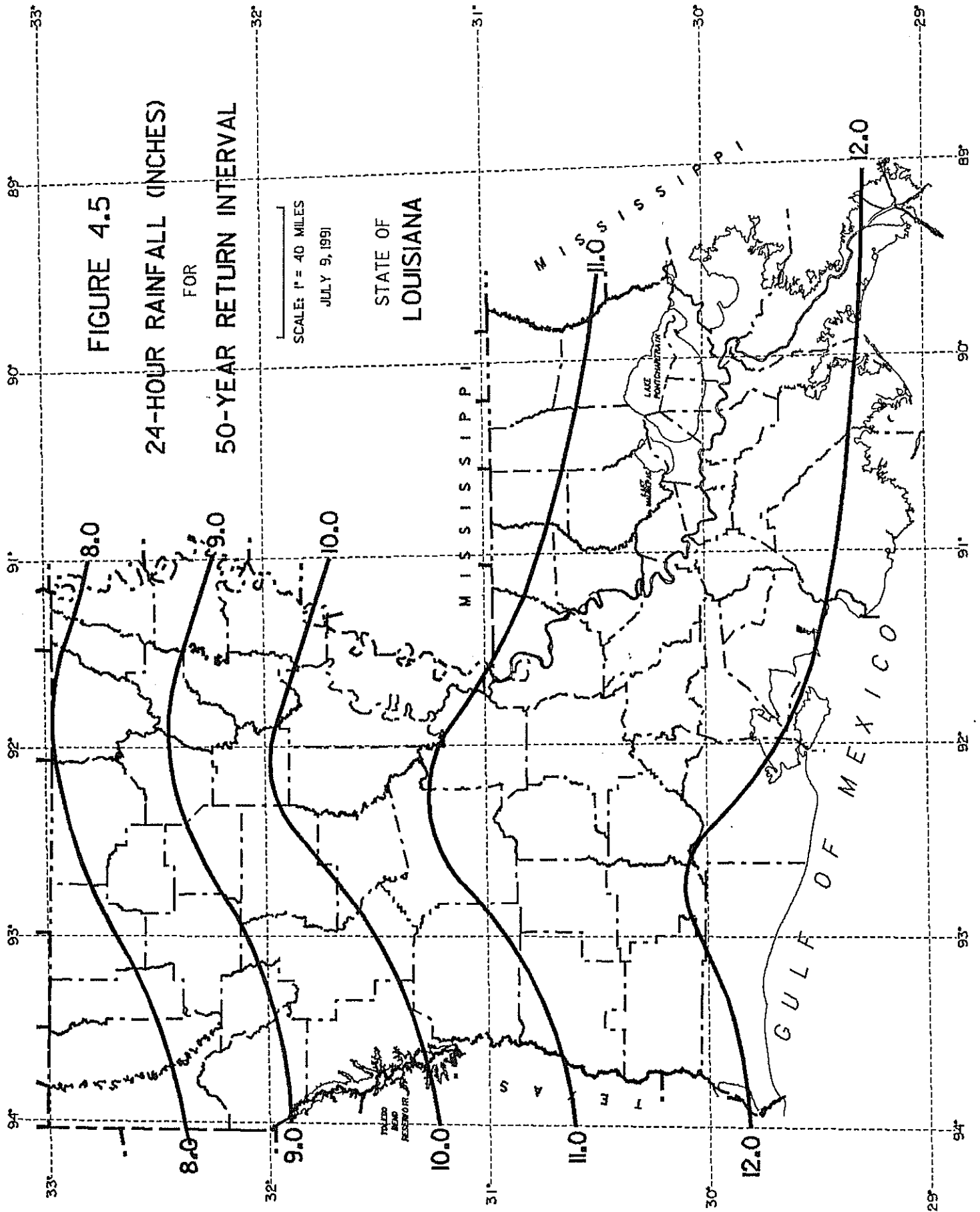


FIGURE 4.3
24-HOUR RAINFALL (INCHES)
FOR
10-YEAR RETURN INTERVAL

SCALE: 1" = 40 MILES
 JULY 9, 1991

STATE OF
 LOUISIANA





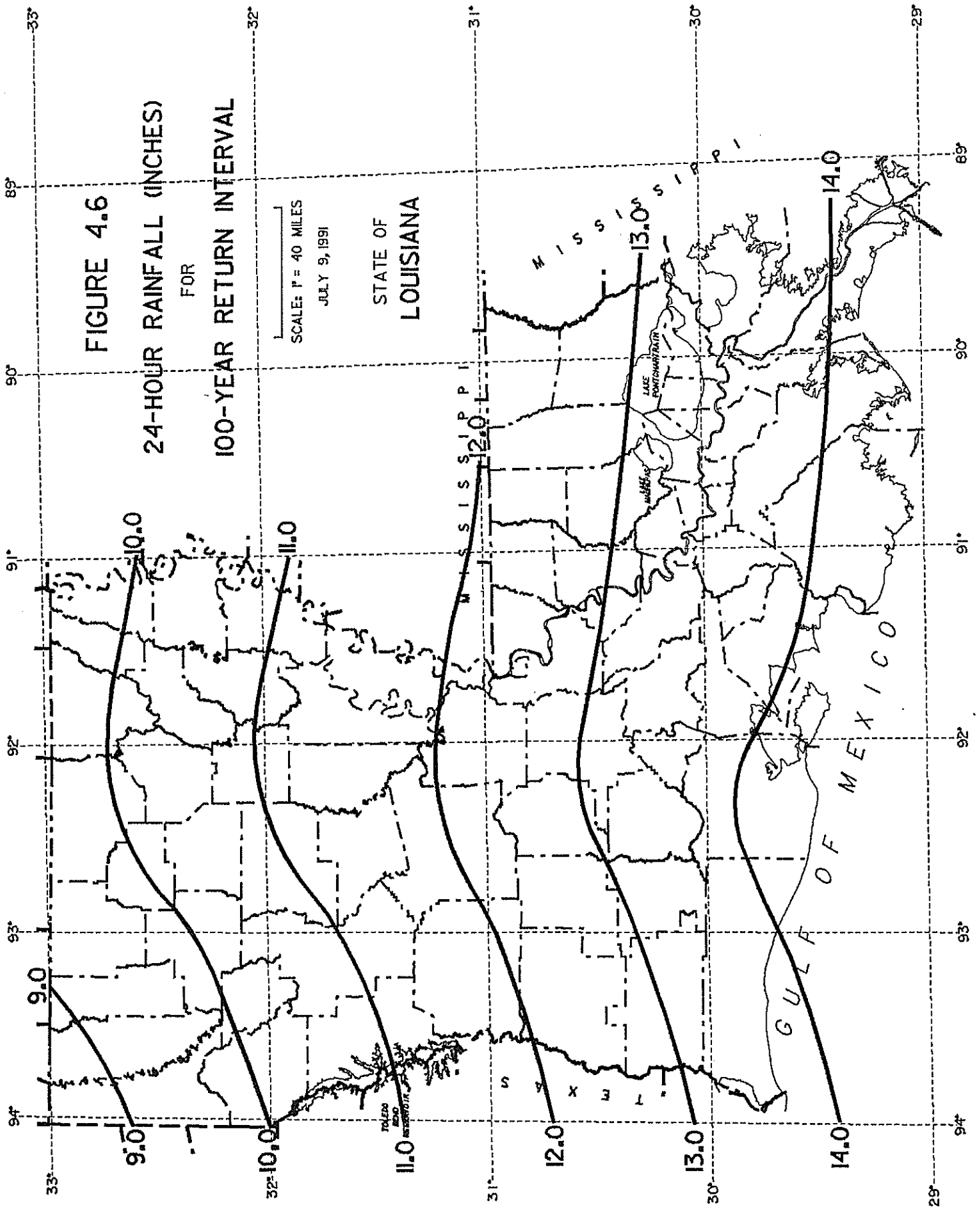


TABLE 5.1
PARAMETERS FOR THE I-D-F GRAPHS WITH RETURN PERIOD OF 2 YEARS

STATION NO.	a	b	c
1	2.885	0.628	-0.847
2	2.387	0.260	-0.771
3	2.698	0.693	-0.866
4	2.768	0.683	-0.841
5	2.878	0.652	-0.872
6	2.833	0.507	-0.826
7	2.366	0.464	-0.763
8	2.659	0.597	-0.793
9	2.588	0.288	-0.793
10	2.747	0.456	-0.806
11	2.754	0.420	-0.805
12	2.245	0.397	-0.794
13	2.154	0.163	-0.756
14	3.197	0.867	-0.889
15	3.707	1.447	-0.918
16	2.387	0.615	-0.815
17	1.995	0.152	-0.788
18	2.838	0.954	-0.883
19	2.181	0.525	-0.810
20	2.090	0.496	-0.847
21	1.640	0.104	-0.770
22	1.948	0.439	-0.787
23	1.700	0.225	-0.762
24	2.108	0.385	-0.801
25	1.948	0.346	-0.789
26	1.765	0.395	-0.719

TABLE 5.2
PARAMETERS FOR THE I-D-F GRAPHS WITH RETURN PERIODS of 5 YEARS

STATION NO.	a	b	c
1	3.859	0.782	-0.828
2	3.354	0.367	-0.790
3	3.001	0.413	-0.793
4	3.484	0.754	-0.808
5	3.438	0.604	-0.817
6	3.495	0.549	-0.794
7	2.682	0.211	-0.724
8	3.432	0.638	-0.771
9	3.351	0.337	-0.791
10	3.761	0.727	-0.990
11	4.121	0.691	-0.818
12	2.709	0.390	-0.751
13	3.841	0.735	-0.836
14	3.481	0.571	-0.816
15	3.794	0.941	-0.841
16	3.437	0.631	-0.805
17	2.145	0.004	-0.736
17	4.490	1.289	-0.923
19	2.998	0.643	-0.831
20	2.913	0.719	-0.837
21	2.104	0.135	-0.763
22	3.161	0.663	-0.831
23	2.415	0.425	-0.783
24	2.753	0.502	-0.778
25	2.651	0.477	-0.779
26	2.754	0.682	-0.778

TABLE 5.3
PARAMETERS FOR THE I-D-F GRAPHS WITH RETURN PERIOD OF 10 YEARS

STATION NO.	a	b	c
1	4.535	0.857	-0.814
2	4.495	0.586	-0.836
3	3.029	0.133	-0.732
4	3.918	0.785	-0.783
5	3.827	0.619	-0.784
6	3.934	0.593	-0.777
7	2.864	0.053	-0.702
8	3.942	0.681	-0.758
9	4.081	0.463	-0.804
10	4.422	0.903	-0.775
11	5.404	1.001	-0.842
12	2.956	0.362	-0.719
13	6.066	1.393	-0.916
14	3.505	0.353	-0.756
15	3.621	0.506	-0.787
16	4.139	0.580	-0.789
17	2.321	-0.014	-0.720
18	5.507	1.377	-0.936
19	3.646	0.749	-0.851
20	3.717	1.005	-0.846
21	2.595	0.297	-0.779
22	4.766	0.917	-0.892
23	3.281	0.761	-0.831
24	3.404	0.677	-0.782
25	3.261	0.653	-0.770
26	3.624	0.652	-0.828

TABLE 5.4
PARAMETERS FOR THE I-D-F GRAPHS WITH RETURN PERIOD OF 25 YEARS

STATION NO.	a	b	c
1	5.472	0.946	-0.799
2	7.036	1.033	-0.928
3	3.049	-0.191	-0.658
4	4.458	0.824	-0.753
5	4.362	0.683	-0.746
6	4.463	0.648	-0.757
7	3.095	-0.117	-0.681
8	4.639	0.768	-0.746
9	5.361	0.714	-0.835
10	5.314	1.156	-0.757
11	7.728	1.547	-0.887
12	3.219	0.312	-0.678
13	12.843	2.789	-1.069
14	3.468	0.089	-0.678
15	3.491	0.074	-0.737
16	5.056	0.489	-0.765
17	2.591	0.002	-0.711
18	6.562	1.374	-0.940
19	4.555	0.883	-0.877
20	5.279	1.580	-0.874
21	3.514	0.647	-0.816
22	8.712	1.351	-1.000
23	5.377	1.485	-0.930
24	4.555	0.991	-0.801
25	4.379	1.047	-0.770
26	5.022	0.494	-0.899

TABLE 5.5
PARAMETERS FOR THE I-D-F GRAPHS WITH RETURN PERIOD OF 50 YEARS

STATION NO.	a	b	c
1	6.211	1.003	-0.789
2	10.504	1.510	-1.021
3	3.086	-0.389	-0.607
4	4.869	0.859	-0.731
5	4.783	0.756	-0.720
6	4.865	0.697	-0.745
7	3.267	-0.224	-0.668
8	5.191	0.849	-0.738
9	6.664	0.963	-0.865
10	6.050	1.381	-0.746
11	10.331	2.097	-0.931
12	3.414	0.282	-0.651
13	-----	-----	-----
14	3.439	-0.086	-0.623
15	3.452	-0.164	-0.709
16	5.777	0.414	-0.746
17	2.827	0.037	-0.709
18	7.219	1.328	-0.938
19	5.322	0.988	-0.897
20	7.285	2.258	-0.914
21	4.596	1.053	-0.860
22	14.552	1.764	-1.103
23	8.657	2.326	-1.038
24	5.859	1.339	-0.829
25	5.723	1.556	-0.785
26	6.410	0.369	-0.959

TABLE 5.6
PARAMETERS FOR THE I-D-F GRAPHS WITH RETURN PERIOD OF 100 YEARS

STATION NO.	a	b	c
1	7.041	1.070	-0.782
2	16.942	2.144	-1.140
3	3.148	-0.548	-0.562
4	5.293	0.901	-0.712
5	5.231	0.850	-0.696
6	5.276	0.752	-0.734
7	3.443	-0.315	-0.657
8	5.803	0.953	-0.734
9	8.370	1.264	-0.899
10	6.864	1.642	-0.736
11	14.247	2.801	-0.987
12	3.601	0.252	-0.626
13	-----	-----	-----
14	3.418	-0.242	-0.571
15	3.458	-0.343	-0.689
16	6.506	0.331	-0.726
17	3.090	0.087	-0.709
18	7.741	1.251	-0.933
19	6.186	1.100	-0.919
20	10.995	3.299	-0.981
21	6.332	1.635	-0.918
22	26.003	2.273	-1.229
23	15.874	3.533	-1.181
24	7.760	1.796	-0.868
25	8.300	2.485	-0.831
26	8.252	0.264	-1.027

Fig. 3.11 Histogram of MAX Annual
24-HR Rainfall Series at Station 10

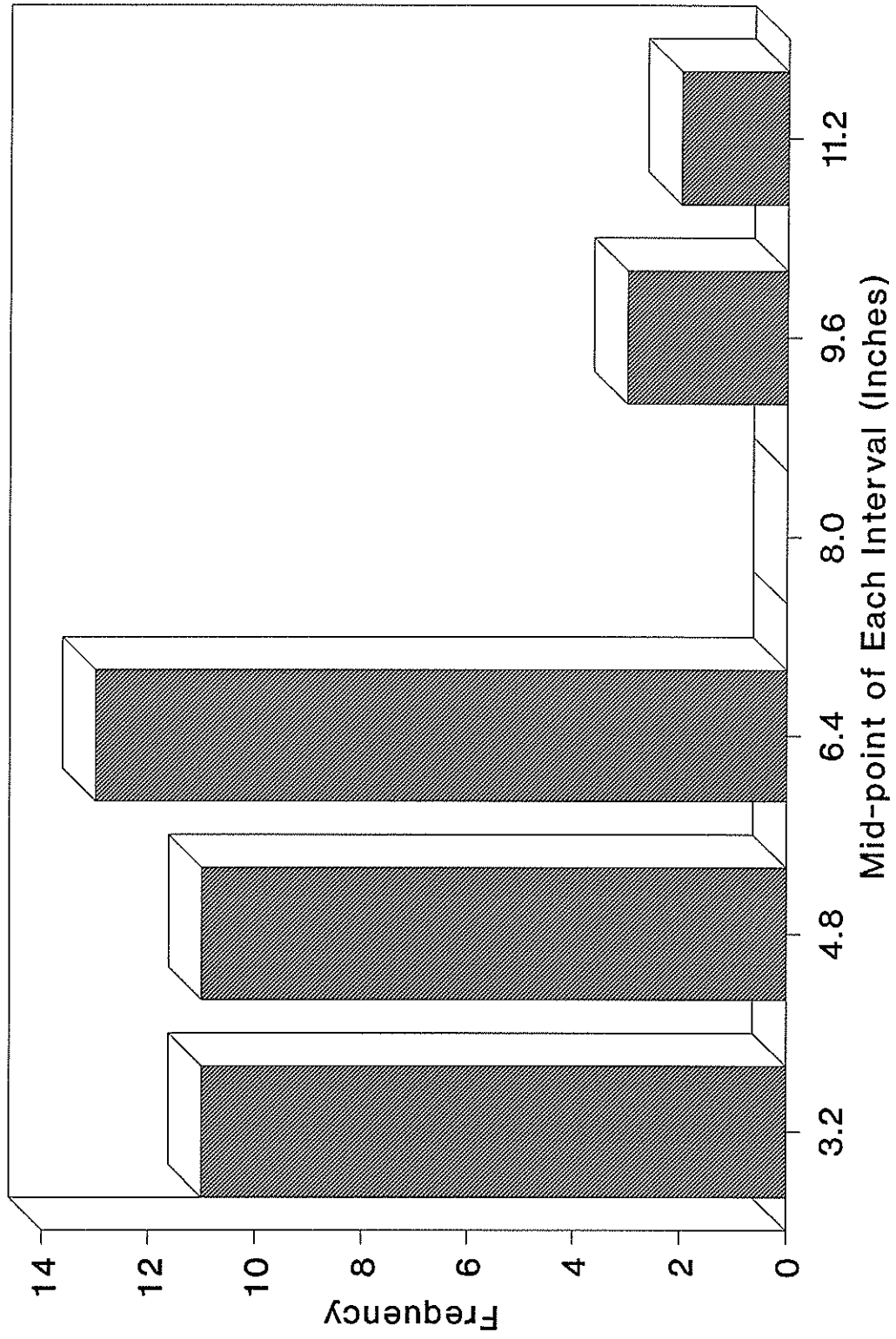
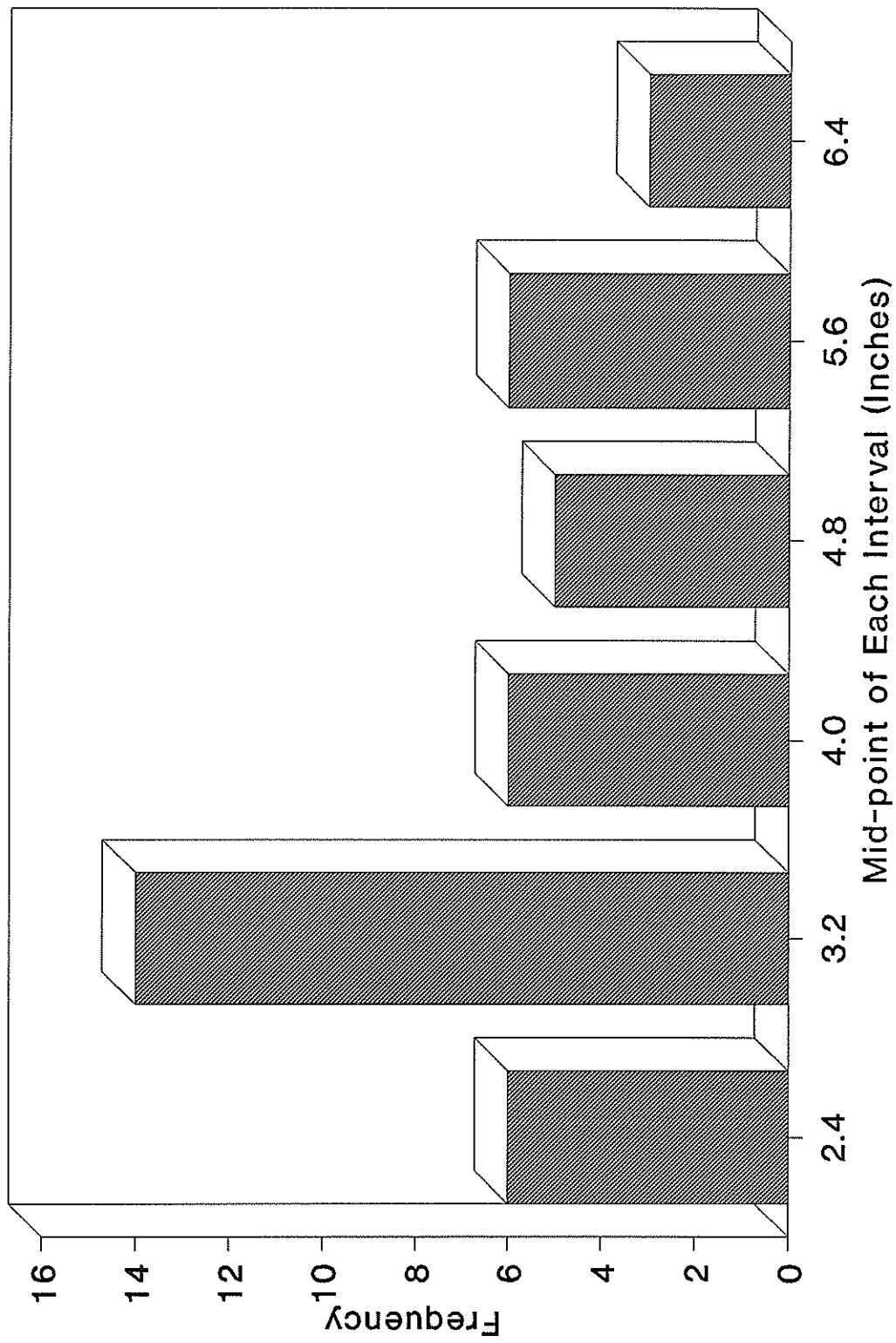


Fig. 3.12 Histogram of MAX Annual
24-HR Rainfall Series at Station 19



3.3 SELECTION OF DISTRIBUTIONS AND PARAMETER ESTIMATION METHODS

A more quantitative approach for selection of an appropriate distribution and parameter estimation method is to test some of the most frequently used distributions in applied hydrology along with the most robust parameter estimation methods. Using certain goodness-test statistics criteria such as mean square error and bias, one can compare the performances of different combinations of the distributions and estimation methods and select the best combination.

In this study, five popular distributions and three parameter estimation methods widely used in applied hydrology were considered for a comparative analysis.

The five probability distributions are:

1. 2-parameter log-normal (LNO2)
2. 3-parameter log-normal (LNO3)
3. Pearson type 3 (PEAR3)
4. log-Pearson type 3 (LPEAR3)
5. Extreme-value type 1 (GUMBEL)

The three parameter estimation methods are:

1. Method of moments (MOM)
2. Maximum-likelihood estimate (MLE)
3. Principle of Maximum entropy (POME)

These five distributions and three estimation methods have been discussed in detail in the literature. Therefore, only a brief summary is given here.

3.3.1 TWO-PARAMETER LOG NORMAL DISTRIBUTION (LNO2)

The probability density function of this distribution is

$$f(x) = \frac{1}{x \sigma_y \sqrt{(2 \pi)}} \text{EXP} \left[- \frac{(\text{LN}(x) - \mu_y)^2}{2 \sigma_y^2} \right], \quad y = \text{LN}(x) \quad (3.3)$$

where x is the rainfall depth variate, $y = \text{LN}(x)$ is the natural log-transformed variable, μ_y and σ_y are the mean and the standard deviation of y . In another form, Equation (3.3) can be expressed as

$$F(y) = \frac{1}{\sigma_y \sqrt{(2 \pi)}} \text{EXP} \left[- \frac{(y - \mu_y)^2}{2 \sigma_y^2} \right], \quad y = \text{LN}(x) \quad (3.4)$$

$f(y)$ is bell-shaped and symmetrical about its mean μ_y with skew coefficient $G_y = 0$. The cumulative distribution function is defined as

$$F(y) = \int_{-\infty}^y \frac{1}{\sigma_y \sqrt{(2 \pi)}} \text{EXP} \left[- \frac{(y - \mu_y)^2}{2 \sigma_y^2} \right] dy, \quad y = \text{LN}(x) \quad (3.5)$$

The parameters of this distribution, μ_y and σ_y , are estimated by the following methods:

1. Method of moments (13)

$$\hat{\mu}_y = \text{LN} \left[\frac{(\hat{\mu}_x)^2}{\sqrt{(\hat{\mu}_x)^2 + (\hat{\sigma}_x)^2}} \right] \quad (3.6)$$

$$\hat{\sigma}_y = \sqrt{\left[\text{LN} \left(1 + \frac{(\hat{\sigma}_x)^2}{(\hat{\mu}_x)^2} \right) \right]} \quad (3.7)$$

where $\hat{\mu}_x$ and $\hat{\sigma}_x$ are the mean and standard deviation of x , defined as

$$\hat{\mu}_x = \frac{1}{n} \sum_{i=1}^n x_i \quad (3.8)$$

$$\hat{\sigma}_x = \sqrt{\frac{1}{(n-1)} \sum_{i=1}^n (x_i - \hat{\mu}_x)^2} \quad (3.9)$$

where n is the number of observations at each synthesized station and x_i is the i -th annual maximum rainfall value.

2. MLE (13)

$$\hat{\mu}_y = \frac{1}{n} \sum_{i=1}^n \text{LN}(x_i) \quad (3.10)$$

$$\hat{\sigma}_y = \sqrt{\frac{1}{(n-1)} \sum_{i=1}^n (\text{LN}(x_i) - \hat{\mu}_y)^2} \quad (3.11)$$

3. POME (14): The same as MLE.

For a given exceedance probability $p(x)$,

$$p(x) = 1 - F(x) = \int_x^{\infty} f(x) dx \quad (3.12)$$

The cumulative probability, F, can be calculated as

$$F = 1 - p(x) \quad (3.13)$$

The return period, T, for a given exceedance probability is calculated as 1/F for $F \leq 0.5$ and as $1/(F-1)$ for $F > 0.5$.

The quantile for a given return period T can be computed as

$$X_T = \text{EXP}(\hat{\mu}_y + t\hat{\sigma}_y) \quad (3.14)$$

where t is the standard normal deviate and is calculated by the following approximation (13) with a maximum possible error of 4.5×10^{-4} . For $F \leq 0.5$,

$$t = -w + \frac{c_0 + c_1 w + c_2 w^2}{1 + d_1 w + d_2 w^2 + d_3 w^3} \quad (3.15)$$

where

$$w = \sqrt{\text{LN}\left(\frac{1}{F^2}\right)} \quad (3.16)$$

and for $F > 0.5$, use $F = p(x)$ in equation (3.16) and take the negative of the value computed by equation (3.15). The coefficients in equation (3.15) are given as

$$C_0 = 2.515517; \quad d_1 = 1.432788$$

$$C_1 = 0.802853; \quad d_2 = 0.189269$$

$$C_2 = 0.010328; \quad d_3 = 0.001308$$

3.3.2 THREE-PARAMETER LOG-NORMAL DISTRIBUTION (LNO3)

The probability density function of the LNO3 distribution is

$$f(x) = \frac{1}{(x-a) \sigma_y \sqrt{2\pi}} \text{EXP} \left[- \frac{(\text{LN}(x-a) - \mu_y)^2}{2\sigma_y^2} \right], \quad 0 \leq a \leq x, \quad y = \text{LN}(x) \quad (3.17)$$

where a is the lower bound of the distribution, and μ_y and σ_y are the mean and standard deviation of the natural logarithms of $(x-a)$.

The parameters of this distribution, a , μ_y and σ_y are estimated by the following methods:

1. MOM (13)

$$\hat{\mu}_y = \frac{1}{n} \sum_{i=1}^n y_i \quad (3.18)$$

$$\hat{\sigma}_y = \sqrt{\frac{1}{(n-1)} \sum_{i=1}^n (y_i - \hat{\mu}_y)^2} \quad (3.19)$$

where $\hat{\mu}_x$ and $\hat{\sigma}_x$ are the mean and standard deviation of x as defined by Equations (3.8) and (3.9).

$$\hat{a} = \hat{\mu}_x - \frac{\hat{\sigma}_x(w)^{1/3}}{1 - (w)^{1/3}} \quad (3.20)$$

where

$$w = \frac{-G_x + \sqrt{(G_x^2 + 4)}}{2} \quad (3.21)$$

and G_x being the coefficient of skewness of the variable x , is computed as

$$G_x = \frac{n \sum_{i=1}^n (x_i - \hat{\mu}_x)^3}{(n-1)(n-2)(\hat{\sigma}_x)^3} \quad (3.22)$$

2. MLE (13)

$$\hat{\mu}_y = \frac{1}{n} \sum_{i=1}^n \text{LN}(x_i - \hat{a}) \quad (3.23)$$

$$\hat{\sigma}_y = \sqrt{\frac{1}{(n-1)} \sum_{i=1}^n [\text{LN}(x_i - \hat{a}) - \hat{\mu}_y]^2} \quad (3.24)$$

$$\sum_{i=1}^n \left[\frac{1}{x_i - \hat{a}} \text{LN}(x_i - \hat{a}) \right] - \sum_{i=1}^n \left[\frac{1}{x_i - \hat{a}} (\hat{\mu}_y - \hat{\sigma}_y^2) \right] = 0 \quad (3.25)$$

The above equations are solved simultaneously by assuming initial values for " \hat{a} " in Equations (3.23) and (3.24).

3. POME (14)

$$\hat{\mu}_y = \frac{1}{n} \sum_{i=1}^n \text{LN}(x_i - \hat{a}) \quad (3.26)$$

$$\hat{\sigma}_y = \sqrt{\frac{1}{(n-1)} \sum_{i=1}^n [\text{LN}(x_i - \hat{a}) - \hat{\mu}_y]^2} \quad (3.27)$$

$$\frac{1}{n} \sum_{i=1}^n (y_i)^4 - \left[\frac{1}{n} \sum_{i=1}^n (y_i)^2 \right]^2 - 2(\hat{\sigma}_y)^2 [2(\hat{\mu}_y)^2 + (\hat{\sigma}_y)^2] = 0, \quad y_i = \text{LN}(x_i - \hat{a}) \quad (3.28)$$

The above equations are solved simultaneously by assuming initial values for " \hat{a} " in Equations (3.26) and (3.27).

By definition, the quantile for a given return period T is computed as

$$X_T = \hat{a} + \text{EXP}(\hat{\mu}_y + t\hat{\sigma}_y) \quad (3.29)$$

where t is calculated, for a given cumulative probability F, from Equation (3.15) along with Equation (3.16).

3.3.3 PEARSON TYPE 3 DISTRIBUTION (PEAR3)

The probability density function of this distribution is

$$f(x) = \frac{1}{a\Gamma(b)} \left(\frac{x-c}{a}\right)^{b-1} \text{EXP}\left(-\frac{x-c}{a}\right), \quad 0 \leq c \leq x \quad (3.30)$$

where a, b and c are the scale, shape and location parameters, respectively. The parameter c is the lower bound of the distribution, and $b > 0$.

The three parameters in the PEAR3 distribution, \hat{a} , \hat{b} and \hat{c} are estimated by the following methods:

1. MOM (13)

$$\hat{a} = \frac{G_x \hat{\sigma}_x}{2} \quad (3.31)$$

$$\hat{b} = \frac{4}{G_x^2} \quad (3.32)$$

$$\hat{c} = \hat{\mu}_x - \hat{a} \hat{b} \quad (3.33)$$

where G_x is the skew coefficient of x . Equation (3.31) is the revised form in this study because the parameter "a" could have a negative value if the coefficient of skew was negative. However, Kite (13) considered "a" to be always positive which implies that the sample skew is also assumed to be always positive.

2. MLE (13)

$$\hat{a} = \frac{S_1 S_2 - n^2}{n S_2} \quad (3.34)$$

where

$$S_1 = \sum_{i=1}^n (x_i - \hat{c}) \quad (3.35)$$

and

$$S_2 = \sum_{i=1}^n \frac{1}{x_i - \hat{c}} \quad (3.36)$$

$$\hat{b} = \frac{S_1 S_2}{S_1 S_2 - n^2} \quad (3.37)$$

$$S_3 - n \psi(\hat{b}) - n \text{LN}(\hat{a}) = 0 \quad (3.38)$$

where

$$S_3 = \sum_{i=1}^n \text{LN}(x_i - \hat{c}) \quad (3.39)$$

and $\Psi(b)$ is the digamma function. Condie and Nix (15) gave an approximate solution as

$$\psi(b) = \frac{\Gamma'(b)}{\Gamma(b)} = \text{LN}(b+2) - \frac{1}{2(b+2)} - \frac{1}{12(b+2)^2} + \frac{1}{120(b+2)^4} - \frac{1}{252(b+2)^6} - \frac{1}{b+1} - \frac{1}{b} \quad (3.40)$$

Matalas and Wallis (16) found that MLE may not always be applicable to PEAR3. They pointed out that

- (a) if sample skew is very small, a solution may not be possible to obtain;
- (b) if $0 < b < 1$, solution is also not possible;
- (c) if $b > 1$, solution is possible only if the sample skew coefficient is less than 2; and
- (d) if skew is negative, the PEAR3 has an upper bound and may not be suitable for at-site frequency analysis. In conclusion, MLE cannot be employed for automatic parameter estimation programs.

TABLE 3.1 (CONT'D.)

RELATIVE MSE OVER 26 STATIONS FOR FIVE DISTRIBUTIONS AND THREE METHODS USING ANNUAL MAXIMUM 24-HOUR RAINFALL SERIES

STA. NO.	METHOD	LNO2	LNO3	PEAR3	LPEAR3	GUMBEL
19	MOM	0.00232	0.00210	0.00199	0.00183	0.00226
	MLE	0.00210	0.00337	0.00400	0.00204	0.00209
	POME	0.00210	0.00391	0.00387	0.00217	0.00198
20	MOM	0.00955	0.00859	0.00736	0.00669	0.01018
	MLE	0.01390	0.02015	0.02186	0.01363	0.01833
	POME	0.01390	0.02188	0.02210	0.01207	0.01418
21	MOM	0.00490	0.00476	0.00461	0.00466	0.00474
	MLE	0.00526	0.00666	0.00730	0.00480	0.00525
	POME	0.00526	0.00718	0.00718	0.00484	0.00493
22	MOM	0.01206	0.00991	0.00846	0.00670	0.01360
	MLE	0.01847	0.02685	0.02926	0.01772	0.02363
	POME	0.01847	0.02899	0.02964	0.01611	0.01912
23	MOM	0.00460	0.00445	0.00425	0.00416	0.00435
	MLE	0.00481	0.00697	0.00773	0.00426	0.00487
	POME	0.00481	0.00761	0.00764	0.00431	0.00456
24	MOM	0.00608	0.00524	0.00446	0.00326	0.00643
	MLE	0.00906	0.01583	0.01776	0.00799	0.01185
	POME	0.00906	0.01739	0.01780	0.00749	0.00936
25	MOM	0.03687	0.02757	0.02803	0.02490	0.04031
	MLE	0.04876	0.05630	0.05893	0.04902	0.05293
	POME	0.04875	0.05939	0.06130	0.04647	0.04778
26	MOM	0.00262	0.00156	0.00155	0.00147	0.00292
	MLE	0.00204	0.00171	0.00195	0.00262	0.00221
	POME	0.00203	0.00171	0.00174	0.00271	0.00227

TABLE 3.2

AVERAGE RELATIVE MSE FOR 26 STATIONS FOR 24-HOUR ANNUAL
MAXIMUM RAINFALL SERIES

		<u>LNO2</u>	<u>LN03</u>	<u>PEAR3</u>	<u>LPEAR3</u>	<u>GUMBEL</u>
MOM	MAX	0.06289	0.05298	0.05722	0.05388	0.06815
	AVG	0.01001	0.00872	0.00843	0.00780	0.01055
	MIN	0.00146	0.00124	0.00119	0.00104	0.00144
MLE	MAX	0.07293	0.08230	0.08704	0.06683	0.07452
	AVG	0.01234	0.01721	0.01885	0.01126	0.01434
	MIN	0.00118	0.00171	0.00195	0.00106	0.00088
POME	MAX	0.07293	0.08677	0.08946	0.07058	0.07262
	AVG	0.01234	0.01859	0.01900	0.01095	0.01255
	MIN	0.00118	0.00129	0.00174	0.00112	0.00098

TABLE 3.3

RELATIVE BIAS FOR EACH STATION USING
ANNUAL MAXIMUM 24-HOUR RAINFALL SERIES

STA. NO.	METHOD	LNO2	LNO3	PEAR3	LPEAR3	GUMBEL
1	MOM	-0.00928	-0.00837	-0.00927	-0.01355	-0.01069
	MLE	-0.01129	0.00039	0.00278	-0.01321	-0.02276
	POME	-0.01129	0.00304	0.00397	-0.01029	-0.01002
2	MOM	-0.00619	-0.00218	-0.00234	-0.00505	-0.00904
	MLE	-0.00624	0.00006	0.00209	-0.00701	-0.01107
	POME	-0.00623	0.00237	0.00332	-0.00720	-0.00924
3	MOM	-0.01066	-0.01310	-0.01476	-0.01806	-0.01195
	MLE	-0.01287	0.00005	0.00220	-0.01604	-0.02386
	POME	-0.01286	0.00283	0.00368	-0.01188	-0.01073
4	MOM	-0.00864	-0.00646	-0.00704	-0.01161	-0.01045
	MLE	-0.01014	0.00033	0.00266	-0.01212	-0.02071
	POME	-0.01013	0.00301	0.00376	-0.00922	-0.01000
5	MOM	-0.01010	-0.01167	-0.01319	-0.01592	-0.01109
	MLE	-0.01261	0.00063	0.00312	-0.01520	-0.02449
	POME	-0.01260	0.00345	0.00420	-0.01158	-0.01005
6	MOM	-0.00781	-0.00564	-0.00614	-0.00887	-0.00993
	MLE	-0.00866	0.00036	0.00254	-0.01041	-0.01605
	POME	-0.00866	0.00278	0.00364	-0.00783	-0.00970
7	MOM	-0.00411	-0.00179	-0.00192	-0.00276	-0.00772
	MLE	-0.00402	0.00011	0.00193	-0.00457	-0.00616
	POME	-0.00401	-0.00342	0.00285	-0.00491	-0.00802
8	MOM	-0.00788	-0.00722	-0.00796	-0.00897	-0.00997
	MLE	-0.00871	0.00033	0.00242	-0.01056	-0.01574
	POME	-0.00870	0.00303	0.00374	-0.01053	-0.00969
9	MOM	-0.00644	-0.00716	-0.00792	-0.01067	-0.00918
	MLE	-0.00780	0.00039	0.00233	-0.00991	-0.01806
	POME	-0.00780	0.00281	0.00346	-0.00718	-0.00870

TABLE 3.3 (CONT'D.)

RELATIVE BIAS FOR EACH STATION USING
ANNUAL MAXIMUM 24-HOUR RAINFALL SERIES

STA. NO.	METHOD	LNO2	LNO3	PEAR3	LPEAR3	GUMBEL
10	MOM	-0.01148	-0.01094	-0.01223	-0.01430	-0.01182
	MLE	-0.01338	0.00015	0.00322	-0.01566	-0.02264
	POME	-0.01338	0.00340	0.00426	-0.01212	-0.01096
11	MOM	-0.01122	-0.01011	-0.01127	-0.01158	-0.01161
	MLE	-0.01227	0.00028	0.00338	-0.01297	-0.01958
	POME	-0.01227	0.00648	0.00428	-0.01269	-0.01089
12	MOM	-0.00766	-0.01415	-0.01611	-0.01262	-0.00986
	MLE	-0.00919	0.00078	0.00242	-0.01143	-0.01425
	POME	-0.00918	0.00293	0.00378	-0.01125	-0.00873
13	MOM	-0.00761	-0.01065	-0.01207	-0.01001	-0.00983
	MLE	-0.00868	0.00057	0.00277	-0.01047	-0.01419
	POME	-0.00867	0.00295	0.00376	-0.00793	-0.00918
14	MOM	-0.01355	-0.02654	-0.01056	-0.02271	-0.01264
	MLE	-0.01613	0.00057	0.00415	-0.01938	-0.01811
	POME	-0.01612	0.000413	0.00499	-0.01520	-0.00960
15	MOM	-0.00732	-0.00525	-0.00565	-0.00563	-0.00999
	MLE	-0.00724	-0.00021	0.00201	-0.00782	-0.01026
	POME	-0.00724	0.00219	0.00326	-0.00818	-0.01010
16	MOM	-0.01481	-0.01313	-0.01479	-0.02425	-0.01316
	MLE	-0.01997	0.00044	0.00359	-0.02310	-0.03728
	POME	-0.01996	0.00346	0.00475	-0.01841	-0.01157
17	MOM	-0.00373	-0.00302	-0.00318	-0.00432	-0.00805
	MLE	-0.00389	-0.00034	0.00151	-0.00582	-0.00763
	POME	-0.00389	-0.00476	0.00206	-0.00651	-0.00825
18	MOM	-0.01062	-0.00934	-0.01031	-0.00638	-0.01162
	MLE	-0.00970	0.00022	0.00235	-0.00829	-0.01349
	POME	-0.00970	0.00299	0.00397	-0.00917	-0.01127

TABLE 3.3 (CONT'D.)

RELATIVE BIAS FOR EACH STATION USING
ANNUAL MAXIMUM 24-HOUR RAINFALL SERIES

STA. NO.	METHOD	LNO2	LNO3	PEAR3	LPEAR3	GUMBEL
19	MOM	-0.00513	-0.00246	-0.00264	-0.00478	-0.00840
	MLE	-0.00532	0.00043	0.00210	-0.00649	-0.01007
	POME	-0.00532	0.00239	0.00310	-0.00680	-0.00856
20	MOM	-0.01078	-0.01243	-0.01396	-0.01968	-0.01190
	MLE	-0.01349	0.00040	0.00201	-0.01594	-0.02740
	POME	-0.01349	0.00308	0.00377	-0.01249	-0.01064
21	MOM	-0.00472	-0.00420	-0.00454	-0.00669	-0.00819
	MLE	-0.00534	0.00062	0.00213	-0.00770	-0.01167
	POME	-0.00534	0.00235	0.00297	-0.00495	-0.00808
22	MOM	-0.01200	-0.01567	-0.01787	-0.02101	-0.01237
	MLE	-0.01500	0.00025	0.00268	-0.01804	-0.02739
	POME	-0.01500	0.00310	0.00416	-0.01390	-0.01078
23	MOM	-0.00588	-0.00465	-0.00504	-0.00664	-0.00885
	MLE	-0.00641	0.00068	0.00202	-0.00779	-0.01192
	POME	-0.00640	0.00265	0.00329	-0.00585	-0.00875
24	MOM	-0.00932	-0.01072	-0.01207	-0.01413	-0.01070
	MLE	-0.01138	0.00065	0.00289	-0.01386	-0.02167
	POME	-0.01138	0.00316	0.00405	-0.01042	-0.00981
25	MOM	-0.001100	-0.02246	-0.01821	-0.02674	-0.01150
	MLE	-0.01466	0.00090	0.00310	-0.01712	-0.02635
	POME	-0.01465	0.00357	0.00447	-0.01394	-0.00876
26	MOM	-0.00440	0.00071	0.00069	-0.00003	-0.00798
	MLE	-0.00352	-0.00160	0.00196	-0.00307	-0.00230
	POME	-0.00351	-0.00061	0.00275	-0.00375	-0.00866

TABLE 3.4

AVERAGE RELATIVE BIAS FOR 26 STATIONS FOR 24-HOUR ANNUAL
MAXIMUM RAINFALL SERIES

		<u>LNO2</u>	<u>LN03</u>	<u>PEAR3</u>	<u>LPEAR3</u>	<u>GUMBEL</u>
MOM	MAX	-0.00373	0.00071	0.00069	-0.00003	-0.00772
	AVG	-0.00855	-0.00918	-0.00924	-0.01181	-0.01033
	MIN	-0.01481	-0.02654	-0.01821	-0.02674	-0.01316
MLE	MAX	-0.00352	0.00090	0.00415	-0.00307	-0.00230
	AVG	-0.00992	0.00029	0.00255	-0.01169	-0.01750
	MIN	-0.01997	-0.00160	0.00151	-0.02310	-0.03728
POME	MAX	-0.00351	0.00413	0.00499	-0.00375	-0.00802
	AVG	-0.00992	0.00232	0.00370	-0.00978	-0.00964
	MIN	-0.01996	-0.00476	0.00206	-0.01841	-0.01157

CHAPTER 4

DEVELOPMENT OF THE 24-HOUR ISOHYETAL MAPS

4.1 INTRODUCTION

One of the objectives of this project was to develop 24-hour isohyetal maps for Louisiana for various return periods. These isohyetal maps are useful for hydrologic design, urban development, soil conservation, highway development, etc. The estimated 24-hour rainfall quantiles were obtained at all 26 stations using LPEAR3 distribution in conjunction with the WRC-recommended estimation method (MOM).

4.2 DEVELOPMENT OF ISOHYETAL MAPS

Rainfall quantiles for the 26 stations for 11 durations (1 through 96 hours) were computed using LPEAR3 distribution with the MOM estimation method. These values are represented in Tables 4.1 through 4.11. Since the observed data sets may contain various errors (which will be discussed in Chapter 6), and may have various lengths of missing records, the estimated quantiles would inevitably contain errors and uncertainties. It was observed that the computed quantiles often changed abruptly from one station to another. Therefore, proper care must be taken for drawing the isohyetal maps. Several rules were devised to make these drawings meaningful.

First, the means of the quantile values were computed from each one-degree quadrangle of latitude and longitude, as shown in Table 4.12, to filter out possible random errors. The "initial" 24-hour isohyetal curves for various return periods were drawn based on these mean values. However, many other types of errors exist which may render the "initial" isohyetal curves unacceptable. As a result, these curves have no distinct pattern and sometimes even intersect each other. To improve the "initial" curves, the following rules were applied:

1. If a station quantile in a one-degree quadrangle deviates from its mean by three standard deviations, that quantile was eliminated from the computed data set.

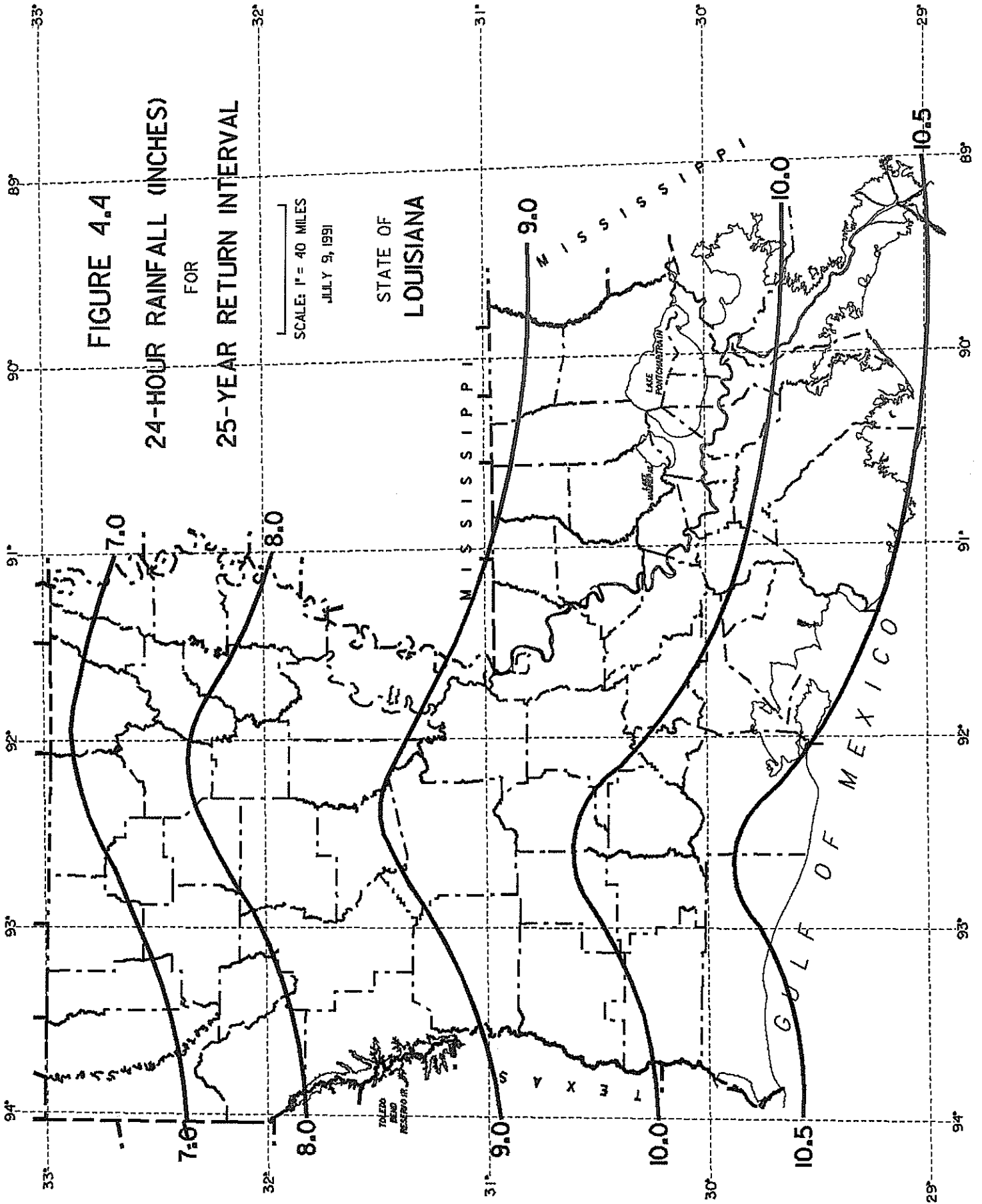
2. If only one or two stations existed in a one-degree quadrangle, adjacent station values were used to compute the mean value.
3. If a station is located between two adjacent one-degree quadrangles, the quantile at that station was used in computations by both one-degree quadrangles.
4. At the corner quadrangles where the trend of the isohyetal lines were unclear, nearby individual station values were given higher importance than average values.
5. When the isohyetal curves changed drastically in a small local area, the curve was modified based on the nearby curve pattern, geographical and climatological conditions, or the reliability of the nearby station data. This was necessary to provide smooth transitions for the isohyetal curves. The final 24-hour isohyetal curves for the return periods $T = 2, 5, 10, 25, 50,$ and 100 years, were drawn based on the above rules, and are shown in Figures 4.1 through 4.6.

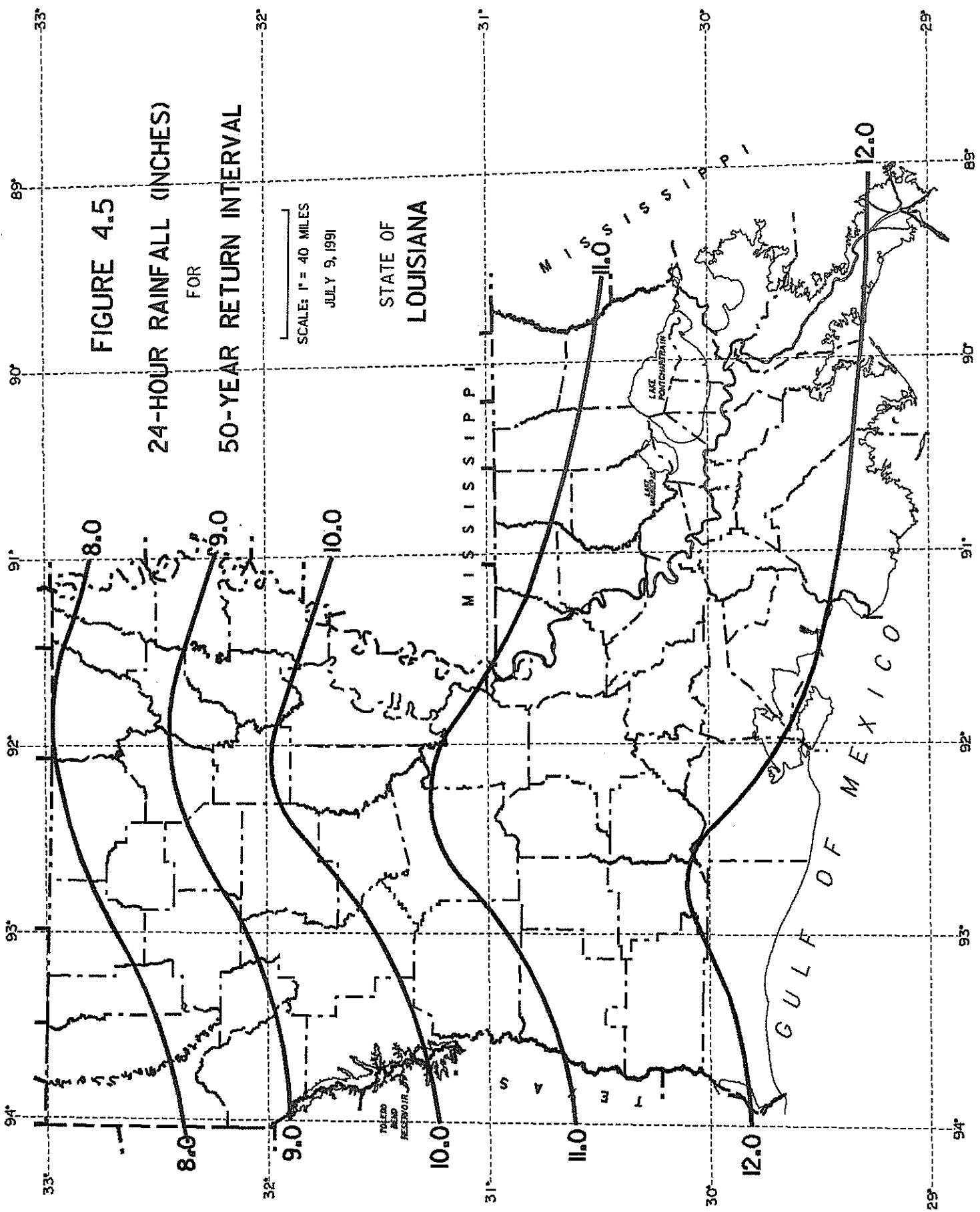
4.3 COMPARISON OF THE NEW MAPS AND TP-40

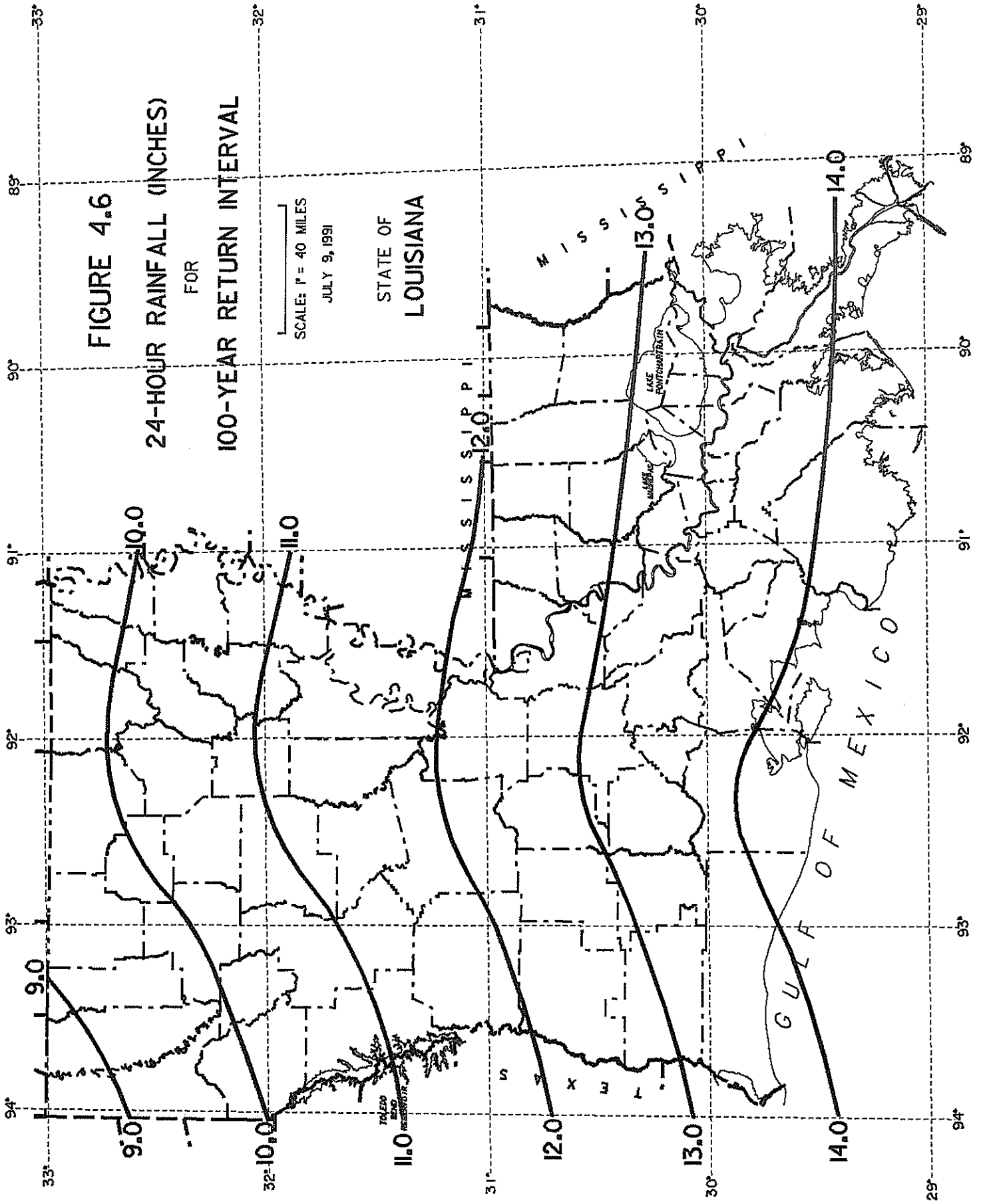
A comparison was made between the newly-developed isohyetal maps ("newmap") and TP-40 for the return periods of 2, 5, 10, 25, 50 and 100 years. The average MSE and BIAS defined by Equations (3.71) and (3.72) were used for the comparison. MSE and BIAS were computed using values from each map at the corresponding stations. Tables 4.13 through 4.18 give the results of the comparison between the TP-40 and the "newmap." The "observed" values are the predicted quantiles from the observed data using LPEAR3-MOM. In general, for return periods of less than or equal to 25 years, the newly-developed isohyetal maps are superior to the TP-40 maps in terms of both MSE and BIAS. For return periods of 50 and 100 years, the newly-developed maps are significantly superior to the TP-40 maps in terms of MSE, but have slightly larger BIAS.

On the average, for all of the 26 synthesized stations corresponding to six return periods, the new maps reduced the MSE by 58 percent and the BIAS by 80 percent, as compared to the TP-

40 maps. Thus, the new isohyetal maps greatly improved the accuracy of the old maps based on the available observed station data.







CHAPTER 5 DEVELOPMENT OF I-D-F CURVES

5.1 INTRODUCTION

The rainfall I-D-F curves are essential tools for design and evaluation of hydraulic structures where a rainfall-runoff model is used. For any rainfall duration and return period (or probability), one can obtain the corresponding rainfall intensity (inches/hour) from the I-D-F curves. The I-D-F curves or models were developed for all 26 stations from the rainfall-intensity quantiles generated using LPEAR3 distribution and the WRC-recommended moment method of parameter estimation.

5.2 DEVELOPMENT OF I-D-F CURVES

At each synthesized station, the 1-, 3-, 6-, 12-, 24-, 36-, 48-, 60-, 72-, 84- and 96-hour quantiles for six return periods ($T = 2, 5, 10, 25, 50$ and 100 years) were calculated by the computer programs discussed in Chapter 2. The corresponding rainfall-intensity quantiles for the above eleven durations and six return periods were also generated using the LPEAR3 distribution in conjunction with the WRC-recommended moment method of parameter estimation. With these computed intensity quantiles for the five durations at each station for each return period, one can fit a model using a non-linear least squares method. The SAS (21) non-linear regression routine was used to fit a model to the computed quantiles. Several models were tested and the following three-parameter non-linear model was selected.

$$I = a (D + b)^c \quad (5.1)$$

where a , b and c are three constant parameters, I is the rainfall intensity (LT^{-1}) for a given return period and D is the rainfall duration (T).

Figures 5.1 and 5.2 show the fitting of three-parameter I-D-F model to the computed values obtained from LPEAR3-MOM and the corresponding for stations number 1 and 24, respectively. The parameters at each station and for different return periods for all 26 stations are given in

Tables 5.1 through 5.6. The parameters changed a great deal from station to station within a given return period. This variation of parameters got larger for higher return periods. This is because errors in the observations increase as the return period is increased. Thus, the I-D-F curves or regression models developed for each single station only represent the estimate of the intensity quantile for a given duration and return period for the immediate vicinity of that station rather than the region. For design purposes, parameters for the station closest to the site should be used with Equation (5.1) to estimate rainfall intensities.

$$S(S_y) = \left[\left(\frac{\partial f(\bar{y}, S_y, G_y)}{\partial S_y} S_y C_v(S_y) \right)^2 \right]^{0.5} \quad (6.30)$$

and for only parameter G_y :

$$S(G_y) = \left[\left(\frac{\partial f(\bar{y}, S_y, G_y)}{\partial G_y} G_y C_v(G_y) \right)^2 \right]^{0.5} \quad (6.31)$$

The partial derivatives with respect to each parameter can be carried out by using Equations (6.15) and (6.18):

$$\frac{\partial f}{\partial \bar{y}} = \text{EXP}(\bar{Y} + K S_y) \quad (6.32)$$

$$\frac{\partial f}{\partial S_y} = K \text{EXP}(\bar{Y} + K S_y) \quad (6.33)$$

$$\begin{aligned} \frac{\partial f}{\partial G_y} = S_y \text{EXP}(\bar{Y} + K S_y) \frac{\partial K}{\partial G_y} = S_y \text{EXP}(\bar{Y} + K S_y) & \left[\frac{t^2 - 1}{6} + \frac{t^3 - 6t}{9} (G_y/6) \right. \\ & \left. - \frac{t^2 - 1}{2} (G_y/6)^2 + \frac{2t}{3} (G_y/6)^3 + \frac{5}{18} (G_y/6)^4 \right] \end{aligned} \quad (6.34)$$

where t can be computed from Equation (6.20).

Based on the estimated parameters from the annual maximum 24-hr rainfall at station 1 for a return period of 50 years by using method of moments, the coefficient of variance for the 50-

year quantile was calculated when the coefficient of variance of each parameter, changed from -1 to +1. The estimated parameters were $\bar{y} = 1.558$, $S_y = 0.3772$, $G_y = 0.5366$, and estimated quantile $X_{50} = 11.44$ inches. Computed results are plotted and shown in Figure 6.1. Output responses to different estimated parameter values are shown in Figures 6.2 through 6.4. It is seen from these figures that the output error is most sensitive to errors in parameter y and secondarily sensitive to parameter S_y , but less sensitive to parameter G_y . Fortunately, the ranks of accuracy in estimating these three parameters are in reverse order of the sensitivity analysis. That is why the moment method of parameter estimation based on the log-transformed data often yields better results.

6.4 FIRST-ORDER ANALYSIS OF UNCERTAINTY FOR RAINFALL-RUNOFF MODELS

Many models have been developed to represent surface runoff as a function of rainfall. One of the most simple yet popular models is the SCS model (25):

$$\begin{aligned}
 Q &= \frac{[P - 0.2(\frac{1000}{CN} - 10)]^2}{P + 0.8(\frac{1000}{CN} - 10)} \\
 &= \frac{(P - \frac{200}{CN} + 2)^2}{P + \frac{800}{CN} - 8}
 \end{aligned}
 \tag{6.35}$$

where P is the rainfall input (inches), Q is the surface runoff depth (inches), and CN is a dimensionless parameter with a value varying from 55 to 98.

Using the equations derived in Section 6.2 for the first-order uncertainty analysis, one can express the variance of Q in terms of the error in the input variable P and parameter CN ,

$$V(Q) = \left[\frac{\partial f(\bar{P}, \bar{CN})}{\partial P} \right]^2 V(P) + \left[\frac{\partial f(\bar{P}, \bar{CN})}{\partial CN} \right]^2 V(CN)
 \tag{6.36}$$

From Equation (6.35)

$$\frac{\partial f(\bar{P}, \bar{CN})}{\partial P} = \frac{2(\bar{P} - \frac{200}{\bar{CN}} + 2)}{\bar{CN}} \cdot \frac{\bar{P} - \frac{200}{\bar{CN}} + 2}{\bar{P} + \frac{800}{\bar{CN}} - 8} - \left[\frac{\bar{P} - \frac{200}{\bar{CN}} + 2}{\bar{P} + \frac{800}{\bar{CN}} - 8} \right]^2 \quad (6.37)$$

and

$$\frac{\partial f(\bar{P}, \bar{CN})}{\partial CN} = \frac{400(\bar{P} - \frac{200}{\bar{CN}} + 2)}{(\bar{CN})^2 (\bar{P} + \frac{800}{\bar{CN}} - 8)} + \frac{\bar{P} - \frac{200}{\bar{CN}} + 2}{(\bar{CN})^2 (\bar{P} + \frac{800}{\bar{CN}} - 8)} \quad (6.38)$$

The coefficient of variation for the runoff can be expressed as a function of the coefficient of variation in input variable P and model parameter CN,

$$C_v(Q) = \frac{1}{f(\bar{P}, \bar{CN})} \left[\left(\frac{\partial f(\bar{P}, \bar{CN})}{\partial P} \bar{P} C_v(P) \right)^2 + \left(\frac{\partial f(\bar{P}, \bar{CN})}{\partial CN} \bar{CN} C_v(CN) \right)^2 \right]^{0.5} \quad (6.39)$$

If the standard error of the output is caused only by the input error in P, then Equation (6.39) may be written as

$$S_Q(P) = \sqrt{\left[\frac{\partial f(\bar{P}, \bar{CN})}{\partial P} \bar{P} C_v(P) \right]^2} \quad (6.40)$$

Similarly, if the standard error of Q is caused only by the error in parameter estimation, Equation (6.39) becomes

$$S_Q(CN) = \sqrt{\left[\frac{\partial f(P, CN)}{\partial CN} \overline{CN} C_V(CN)\right]^2} \quad (6.41)$$

Since $CV(P)$ and $CV(CN)$ represent the relative error of input P and of parameter CN , it is clear that the magnitude of the standard error in output Q linearly depends on the relative error in the input variable and the parameter. The relative importance of the input and the parameter to the contribution of the standard error in output depends on the estimated value CN , observed value P , and their derivatives.

The relative error of output Q in response to the relative error in input P and relative error in parameter CN are calculated over four sets of P and CN values. These results are plotted on Figures 6.5 through 6.7. These plots show that the output is almost equally sensitive to both the input component P and the parameter CN . Therefore, both P and CN must be obtained with great accuracy.

Figure 6.1 First-Order Error Analysis
 Relative Error in 50-YR LPEAR3 Quantile
 Versus Relative Error in Each Parameter

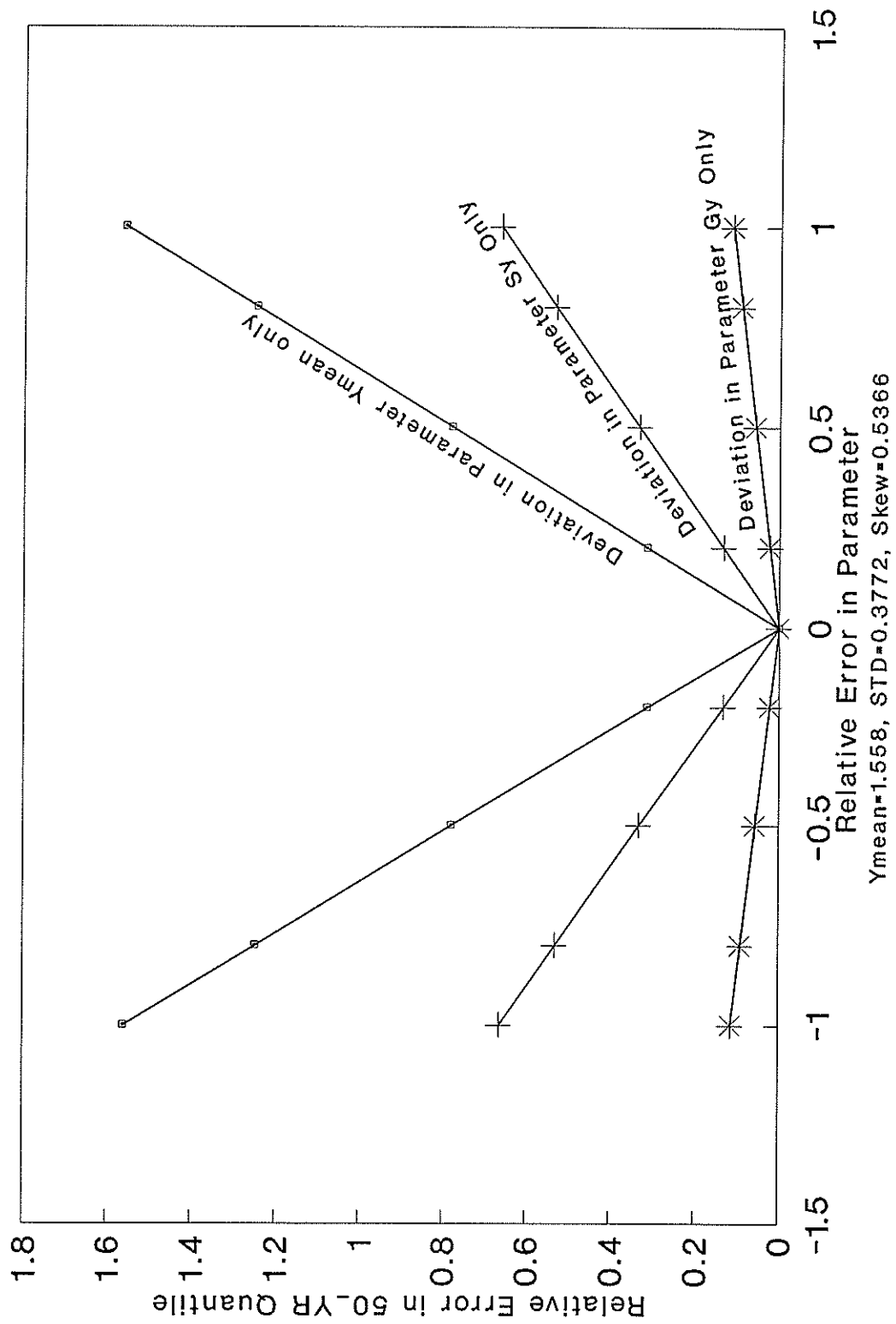


Figure 6.2 First-Order Error Analysis
 Relative Error in 50-YR LPEAR3 Quantile
 Versus Relative Error in Each Parameter

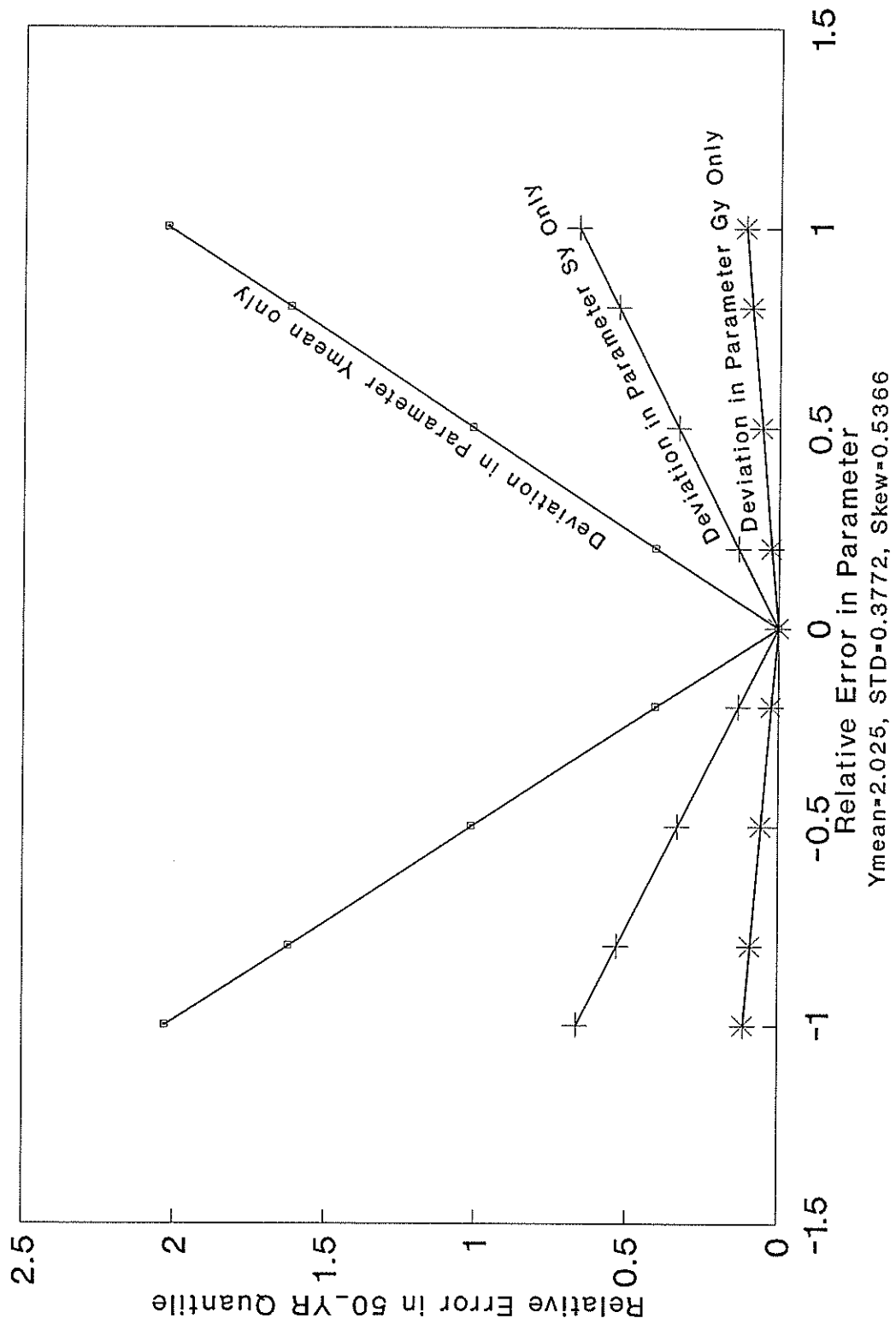


Figure 6.3 First-Order Error Analysis
 Relative Error in 50-YR LPEAR3 Quantile
 Versus Relative Error in Each Parameter

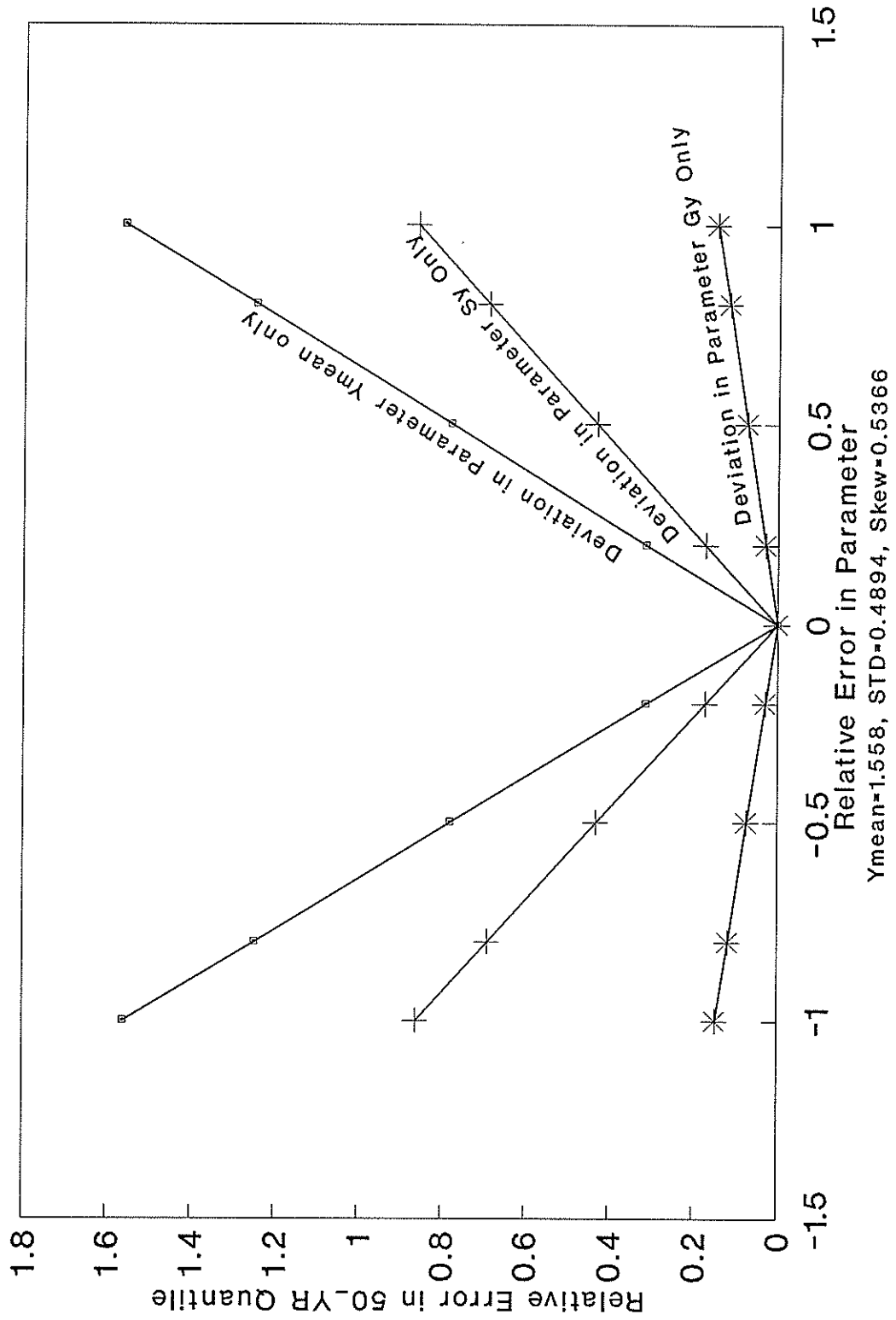


Figure 6.4 First-Order Error Analysis
 Relative Error in 50-YR LPEAR3 Quantile
 Versus Relative Error in Each Parameter

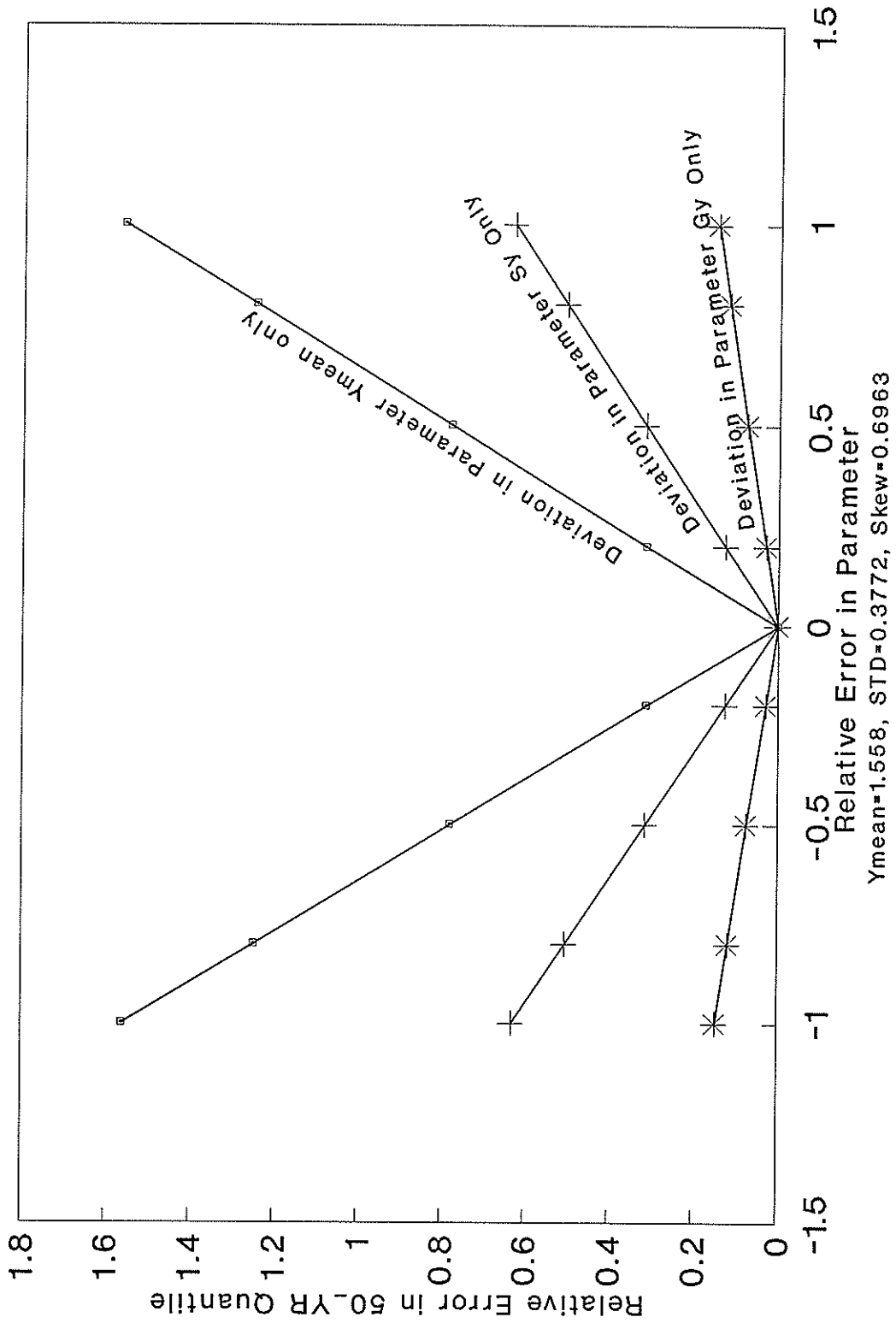


Figure 6.5 First-Order Error Analysis
 Relative Error in Runoff Versus
 Relative Error in Parameter and Rainfall

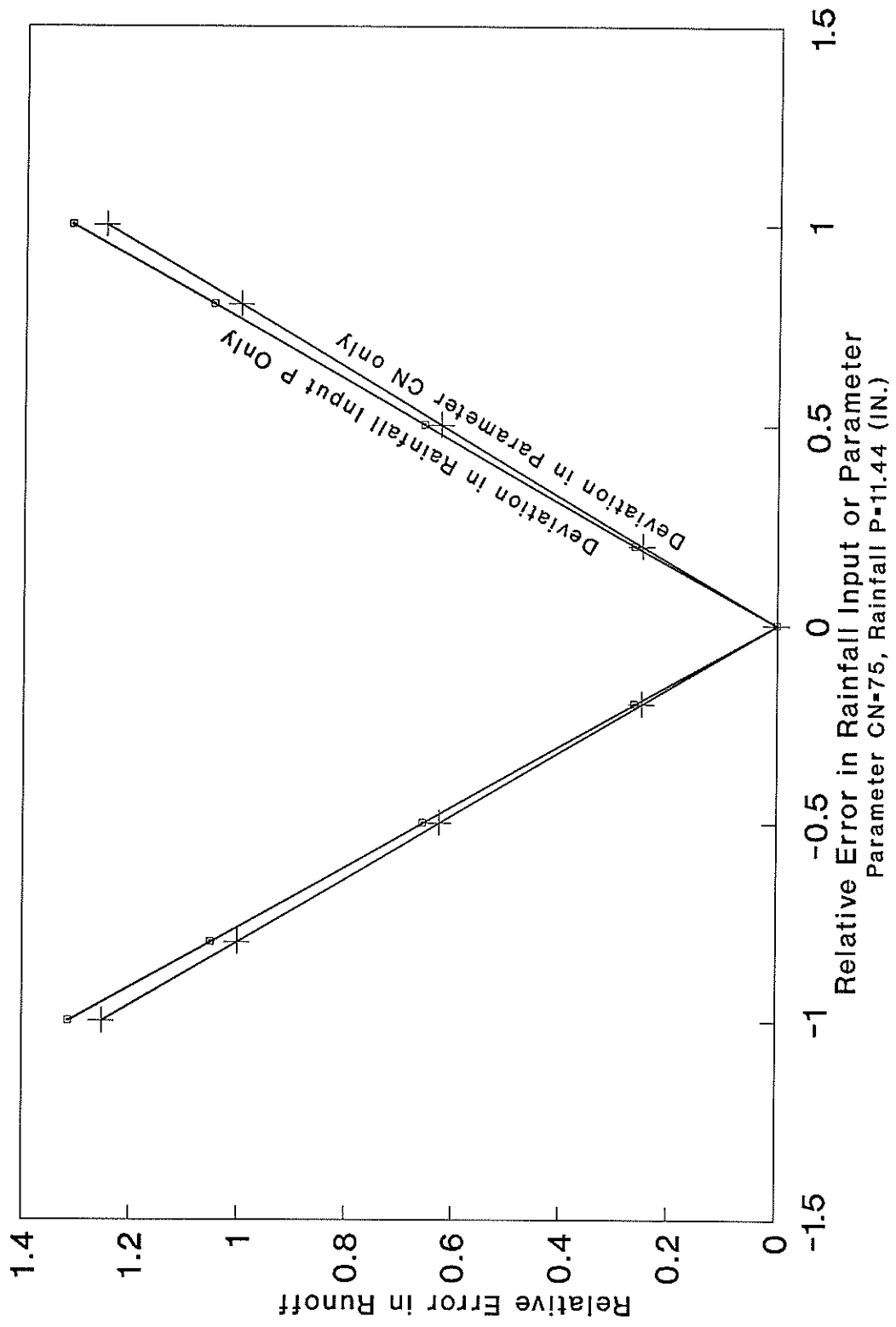


Figure 6.6 First-Order Error Analysis
 Relative Error in Runoff Versus
 Relative Error in Parameter and Rainfall

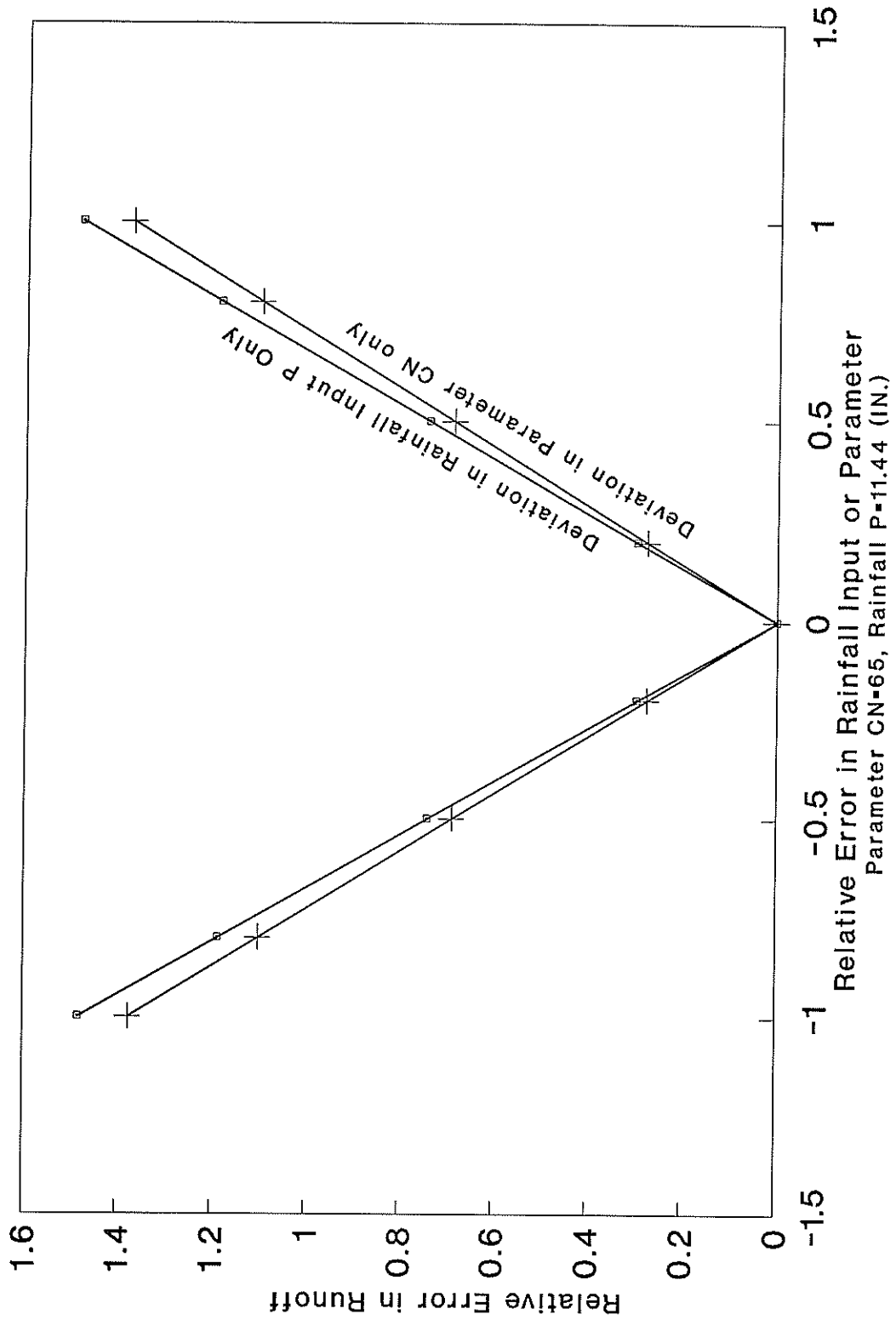
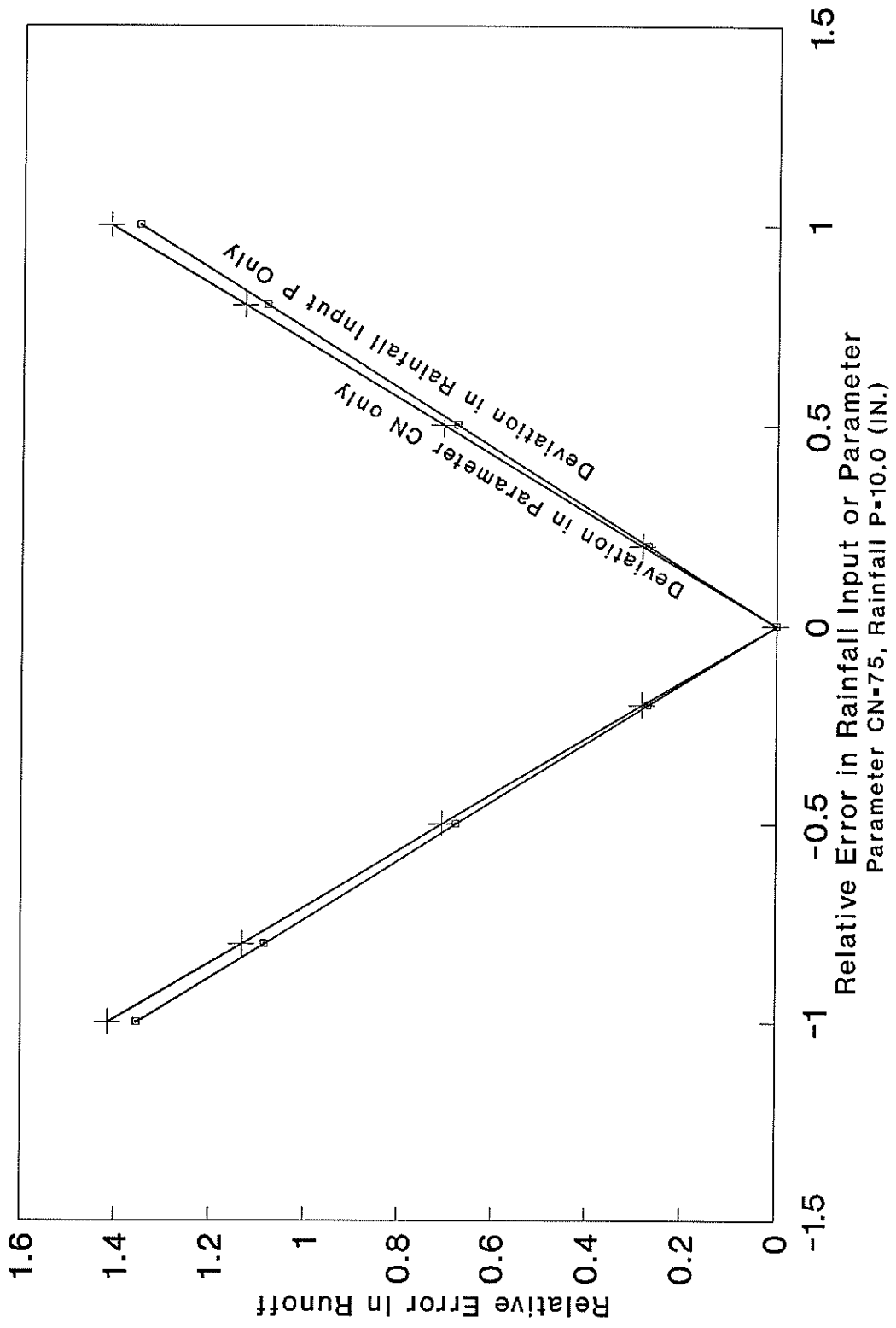


Figure 6.7 First-Order Error Analysis
 Relative Error in Runoff Versus
 Relative Error in Parameter and Rainfall



REFERENCES

1. "Rainfall Frequency Atlas of the United States," Technical Paper No. 40, U.S. Department of Commerce, Washington, D.C., 1961.
2. Yarnell, D. L., "Rainfall-Intensity-Frequency Data", Miscellaneous Publications No. 204, U.S. Department of Agriculture, Washington, D.C., 1935.
3. "Five- to 60-Minute Precipitation Frequency for the Eastern and Central United States," NOAA Technical Memorandum NWS HYDRO-35, National Weather Service, Silver Spring, Md., 1977.
4. Aron, G., et al., Pennsylvania Department of Transportation Storm Intensity-Duration-Frequency Charts, FHWA-PA-85-032, Pennsylvania State University, University Park, Pennsylvania, 1986.
5. "Storm Rainfall Probability Atlas for Arizona," FHWA-AZ88-276, Arizona Department of Transportation, Phoenix, Arizona, 1988.
6. Louisiana Rainfall, Intensity-Duration-Frequency Data and Depth-Area-Duration Data, Department of Public Works, Baton Rouge, Louisiana, 1952.
7. Arora, K. and Singh, V. P., "A Comparative Evaluation of the Estimators of the Log Pearson Type 3 Distribution," Journal of Hydrology, Vol. 105, 1989, pp. 19-37.
8. Kuczera, G., "Robust Flood Frequency Models," Water Resources Research, Vol. 18, No. 2, 1982, pp. 315-324.
9. U.S. Water Resources Council, "Guidelines for Determining Flood Flow Frequency," Hydrology Subcommittee, Bulletin #15, Washington, D.C., 1967.
10. Wallis, J. R., and Wood, E. F., "Relative Accuracy of Log Pearson III Procedures," Journal of the Hydraulics Division, ASCE, Vol. 111, No. HY7, 1985, pp 1043-1056.
11. Arora, K. and Singh, V. P., "On Statistical Intercomparison of EV1 Estimates by Monte Carlo Simulation," Advanced Water Resources, Vol. 10, 1987, pp. 87-107.
12. Jain, D. and Singh, V. P., "Comparison of Some Flood Frequency Distributions Using Empirical Data," Hydrologic Frequency Modeling, V. P. Singh (editor), D. Reidel Co., Germany, 1987, pp. 467-485.
13. Kite, G. W., Frequency and Risk Analysis in Hydrology, Water Resources Publications, P. O. Box 303, Fort Collins, Colorado 80522, 1978.

14. Singh, V. P.; Rajagopal A. K.; and Singh, K., "Derivation of Some Frequency Distributions Using the Principle of Maximum Entropy (POME), *Advanced Water Resources*, Vol. 9, 1986, pp. 91-106.
15. Condie, R. and Nix, G., "Modeling of Low Flow Frequency Distributions and Parameter Estimation," *International Water Resources Association, Proceedings of Symposium on Water for Arid Lands*, Tehran, Dec. 8-9, 1975.
16. Matalas, N. C. and Wallis, J. R., "Eureka, It Fits a Pearson Type 3 Distribution," *Water Resources Research*, Vol. 9, No. 2, 1973, pp. 281-289.
17. Reich, B. M., "Log-Pearson Type 3 and Gumbel Analysis for Floods," *Second International Symposium in Hydrology*, Fort Collins, Colorado, 1972, pp. 290-303.
18. Bobee, B., "The Log-Pearson Type 3 Distribution and its Application in Hydrology," *Water Resources Research*, Vol. 11, No. 5, 1975, pp. 681-689.
19. Rao, D.V., "Log-Pearson Type 3 Distribution: A Generalized Evaluation," *Journal of Hydraulic Engineering*, ASCE, Vol. 106, No. 5, 1980, pp. 853-872.
20. Bobee, B. and Robitaille, R., "The Use of Pearson Type 3 and Log-Pearson Type 3 Distribution Revisited," *Water Resources Research*, Vol. 13, No. 2, 1976, pp. 427-443.
21. SAS User's Guide, Version 5 Edition, SAS Institute Inc., Cary, NC., 1989.
22. Singh, V.P., Hydrologic Systems, Volume I, Rainfall-Runoff Modeling. Prentice Hall, Englewood Cliffs, New Jersey 07632, 1988.
23. Von Neumann, J. and Goldstine, J. J., "Numerical Inverting of Matrices of High Order," *Bulletin of the American Mathematical Society*, Vol. 53, 1947, pp. 1021-99.
24. Singh, V. P. and Yu, F. X., "Derivation of an Infiltration Equation Using Systems Approach," *Journal of Irrigation and Drainage Engineering*, ASCE, Vol. 116, No. 6, 1990, pp. 837-858.
25. Soil Conservation Service National Engineering Handbook, Section 4, Hydrology, U.S. Soil Conservation Service, 1972.